(4)

CHEMICAL RESEARCH, DEVELOPMENT & ENGINEERING CENTER

CRDEC-CR-88033

SPECTROSCOPY OF NON-AGGLOMERATED PARTICLES IN THE CONDENSED PHASE

by Donald R. Huffman

UNIVERSITY OF ARIZONA
Tuscon, AZ 85721

February 1988

U.S. ARMY ARMAMENT MUNITIONS CHEMICAL COMMAND

Aberdeen Proving Ground, Maryland 21010-5423

Disclaimer

The findings in this report are not to be construed as an official Department of the Army position unless so designated by other authorizing documents.

Distribution Statement

Approved for public release; distribution is unlimited.

UNCLASSIFIED
SECURITY CLASSIFICATION OF THIS PAGE

REPORT DOCUMENTATION PAGE

1a REPORT SECURITY CLASSIFICATION UNCLASSIFIED	1b RESTRICTIVE MARKINGS AD-A190662
2a SECURITY CLASSIFICATION AUTHORITY	3 DISTRIBUTION/AVAILABILITY OF REPORT Approved for public release; distribution is unlimited.
2b DECLASSIFICATION/DOWNGRADING SCHEDULE	
4 PERFORMING ORGANIZATION REPORT NUMBER(S) CRDEC-CR-88033	5 MONITORING ORGANIZATION REPORT NUMBER(S)
6a NAME OF PERFORMING ORGANIZATION University of Arizona 6b OFFICE SYMBOL (If applicable)	7a NAME OF MONITORING ORGANIZATION
6c ADDRESS (City, State, and ZIP Code) Tuscon, AZ 85721	7b ADDRESS (City, State, and ZIP Code)
8a NAME OF FUNDING/SPONSORING ORGANIZATION CRDEC 8b OFFICE SYMBOL (If applicable) SMCCR-RSP-B	9 PROCUREMENT INSTRUMENT IDENTIFICATION NUMBER DAAK11-83-K-0014
8c ADDRESS (City, State, and ZIP Code) Aberdeen Proving Ground, MD 21010-5423	10 SOURCE OF FUNDING NUMBERS PROGRAM ELEMENT NO. / PROJECT NO. / TASK NO. / WORK UNIT ACCESSION NO.

11 TITLE (Include Security Classification)
Spectroscopy of Non-Agglomerated Particles in the Condensed Phase

12 PERSONAL AUTHOR(S)
Huffman, Donald R.

13a TYPE OF REPORT	13b TIME COVERED	14 DATE OF REPORT (Year, Month, Day)	15 PAGE COUNT
Contractor	FROM 83 Sep TO 86 Dec	1988 February	63

16 SUPPLEMENTARY NOTATION
COR: Robert Frickel, SMCCR-RSP-B, (301) 671-3854

17 COSATI CODES		
FIELD	GROUP	SUB-GROUP
15	06	03

18 SUBJECT TERMS (Continue on reverse if necessary and identify by block number)
Small particles, Smoke, Extinction, Carbon
Matrix isolation, Clusters, Scattering,

19 ABSTRACT (Continue on reverse if necessary and identify by block number)

Because the optical properties of very small particles are frequently dominated by almost-unavoidable clustering of particles, this work has attempted to study the spectroscopy of systems of particles growing from one atom through multi-atom clusters to small particles. The techniques used are (1) low temperature matrix isolation spectroscopy in solid argon, and (2) in situ study of metal particles produced and growing in an inert gas. In order to help clarify the issue regarding the size regime at which bulk optical properties cease to be a valid approximation for increasingly small particles, Part I surveys this question, based both on the present results and on the work of many authors published in the open literature.

Part II gives more specific details on the matrix isolation and gas phase spectroscopy. Matrix isolation results are given for mixed metal clusters in the
(continued on reverse)

20 DISTRIBUTION/AVAILABILITY OF ABSTRACT	21 ABSTRACT SECURITY CLASSIFICATION
☒ UNCLASSIFIED/UNLIMITED ☐ SAME AS RPT ☐ OTIC USERS	UNCLASSIFIED

22a NAME OF RESPONSIBLE INDIVIDUAL	22b TELEPHONE (Include Area Code)	22c OFFICE SYMBOL
SANDRA J. JOHNSON	(301) 671-2914	SMCCR-SPS-T

DD FORM 1473, 84 MAR 83 APR edition may be used until exhausted
All other editions are obsolete

SECURITY CLASSIFICATION OF THIS PAGE
UNCLASSIFIED

19. ABSTRACT (continued)

Clusters of carbon atoms, presumably up to about 9 atoms in a cluster, are shown to give a rich spectrum of absorption in the visible and UV. Both wavelength-dependent extinction and scattering measurements are shown for silver smoke. A disappointment in the current work, which has been shared by others, is the inability to follow the transition from molecular to solid state spectra above a few atoms for metals and about 9 atoms for carbon.

PREFACE

The work described in this report was authorized under Contract No. DAAK11-83-K-0014. This work was started in September 1983 and completed in December 1986.

The use of trade names or manufacturers' names in this report does not constitute an official endorsement of any commercial products. This report may not be cited for purposes of advertisement.

This report has been approved for release to the public.

Blank

CONTENTS

SPECTROSCOPY OF NON-AGGLOMERATED PARTICLES IN THE CONDENSED PHASE

(CONTENTS CONTINUED)

SPECTROSCOPY OF NON-AGGLOMERATED PARTICLES IN THE CONDENSED PHASE

The experimental study of optical properties of very small particles is frequently dominated by almost-unavoidable clustering of particles. Thus the resulting optical absorption (for example) is quite different from that of individual particles. Unfortunately, this problem is not often recognized. The goal of this three year project has been to apply low temperature matrix isolation spectroscopy to systems of particles growing from one atom through multi-atom clusters to small particles, thus attempting to bridge the gap between molecular and solid state spectroscopy.

One of the sub-goals of this work, as stated in the original proposal, has been, "to help clarify the size regime at which bulk optical properties cease to be a valid approximation for increasingly small particles." Since the Army Program has been particularly interested in this complex issue, Part I of this report is a general addressing of the bulk optical constants issue, both from the present work and from the work of many authors who have published work in the open literature bearing on the problem. Our conclusions are stated on the bottom line of Part I.

Part II gives more details of our work. In particular, it is reported how an additional system for investigating the growth of particles from atomic vapor in the gas phase has been developed. This provides a complementary method to the low temperature matrix isolation.

Part I
THE APPLICABILITY OF BULK OPTICAL CONSTANTS TO SMALL PARTICLES

1. INTRODUCTION

The optical properties of small particles and liquid droplets are of considerable importance in many areas of applied science. Particles in our atmosphere have an impact on climate as well as contributing to the beauty of our sunsets. Particles of all types flow through the blood vessels of our bodies -- lymphocytes, viruses, and many others both friend and foe. Our oceans are full of plankton and other microorganisms. Atmospheres of planets are filled with a variety of particulates, and interplanetary and interstellar space is populated with dust. In this volume several optical effects of small particles are considered, which have become of particular interest in recent years. In all these cases it is usually desirable to model optical effects by calculations of absorption, scattering, etc. The input for such calculations,

along with size and shape information, is usually optical constants — those numbers which describe the frequency-dependent optical response of matter to electromagnetic waves. Sometimes these optical constants are derived from simple models, but more frequently they are taken from experimental determinations. Sometimes the parameters are well known; at other times they can be only roughly approximated. There are numerous situations in which the optical constants are inapplicable to the problem at hand, a size range below which optical constants are inaccurate, and a further small size range in which the entire concept of optical constants loses its validity. Because of the widespread use of optical constants in small-particle optical studies, it is important to understand when the available optical constants for bulk matter are applicable and when they are not.

1.1 Bulk Optical Constants and Small-Particle Optical Properties

It is abundantly clear that the optical properties of solids are qualitatively different from the optical properties of their consitituent atoms and molecules when isolated. A collection of silver atoms in space would clearly have a different absorption spectrum than a silver spoon, even with the tarnish perfectly removed. The often-posed question, however, is where in a decreasing size range of particles (starting with the ~15 cm size of the silver spoon particle, and decreasing toward an ultimate small size of one silver atom), do the bulk optical properties as represented by optical constants cease to be valid? (Exact definitions of optical constants are given in Section 2.1.) Unfortunately, there does not seem to be one simple answer to this question. A large part of this chapter is devoted to the identification of effects which may invalidate the use of bulk optical constants. Before discussing some real deviations in Section 4, we point out a few false alarms that have occurred along the way, caused by the serious difficulty of dealing with clumps of particles. Some examples taken from our own work in carrying out the program of Figure 1 are discussed in Section 5. These include a solid with the mineralogical name of olivine, carbon, and silver, representing a fairly normal metal. Based on these examples and other published results, we summarize in Section 6, with the optical effects found in a thought experiment on particles growing from single atoms through large clusters into small particles and eventually into bulk solids. Conclusions can then be stated to answer the question regarding approximately where bulk optical constants are valid and when they are not.

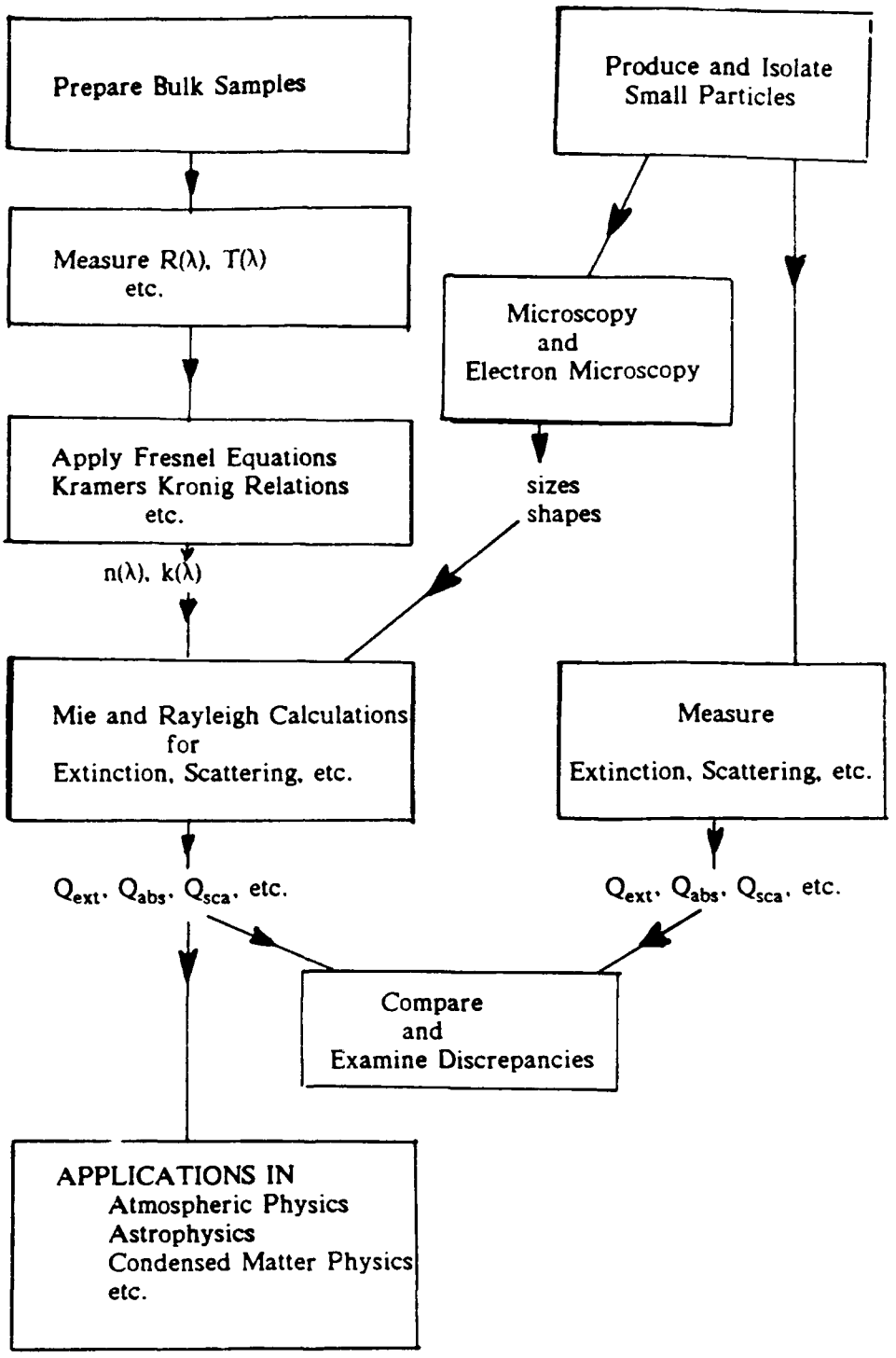

Figure 1. Overview of a program to relate measured and calculated optical properties of small particles.

1.2 A Program to Relate Bulk and Particulate Optical Properties

Optical properties of particulates that are frequently of interest include, for example, the angular dependence of scattering including various possible polarization combinations, the wavelength-dependent absorption and scattering cross sections, and the spectral emissivity. It is possible to measure these optical properties directly, but the results are only appropriate for the specific sample measured -- the identical size and shape distribution of particles including their state of aggregation. It is usually easier to calculate these properties assuming certain simple models for the particle shape, such as spherical or spheroidal, using optical constants as input. A great advantage of being able to calculate optical properties is that one can easily change parameters in the calculation, such as the mean size or size distribution width. A size change in a calculation might require anywhere from a few seconds on up, whereas the equivalent change in an experimental system of small particles might require years to accomplish in the laboratory. Small wonder then that there are so many Mie calculations and so few good experiments. Since many real world particles do not quite conform to spherical models, for example, one would like to be confident that such calculations accurately describe the optical properties of the real particles. A program to accomplish this goal and much more along the way is blocked out in Figure 1. We have followed this plan for a number of years in our laboratory in Tucson. Many other workers have contributed to this sort of synthesis, although not many have undertaken the entire mission set out here.

The left-hand column describes a program to enable one to calculate optical properties of small particles by providing "measured" optical constants. Of course one never "measures" optical constants directly. We have no such instrument as an optical constants meter. One must make measurements such as transmission and reflectance and interpose a suitable theory in order to extract optical constants. These measurements are often far from trivial, as we discuss at more length in Sections 2.2 and 2.3. The bulk samples must first be prepared appropriately, such as by cutting and polishing one or more surfaces. For anisotropic solids, x-ray orientation may be required, and several suitably oriented specimens must be prepared. Measurements such as reflectance and transmittance vs. wavelength are made and appropriate models are applied, such as Fresnel's equations and Kramers-Kronig relations. The results are the "measured" optical constants. These can be used in Mie calculations, for example, to arrive at small-particle absorption and scattering efficiencies and other small-

particle properties. At this point, certain applications of the results are possible. One can relate them to atmospheric effects, observations in astrophysics, condensed matter, etc. Because of our capability for determining optical constants, we have enjoyed the opportunity to have the first try at relating optical properties of certain materials to interesting features of remote particles in interstellar space of unknown composition. Usually no great discoveries come out of this, but it is pleasant to be able to engage in the whole process before passing the basic optical constants on through publication or private correspondence.

To the confirmed experimentalist who lives with the fact that the world is not filled with perfect little homogeneous spheres, the validity of these results and their consequences must be continually questioned, however. Because of this doubt it has seemed important to us to attempt to make small particles of known composition directly, characterize them as to their size, shape, degree of crystallinity, etc., and directly measure their scattering and absorbing properties. This is the small-particle part of the program, outlined in Figure 1 on the right. The size and shape results from microscopy can be fed over to the calculational side to provide calculated values for the corresponding measured quantities. At this point one can compare measured and calculated optical properties of the experimental system and see how well they agree. In many cases they disagree badly. In fact, in the majority of cases we have dealt with, the agreement is bad enough that one is not inclined to make serious use of the calculational process for critical applications. What has gone wrong? Unfortunately there are many possible answers, involving both the left and the right of the diagram. Much of the rest of this chapter deals with things that go wrong. But it is the things that go wrong in the process, the things we obviously do not fully understand, that are the most interesting, for it is here that we may increase our understanding of the real nature of optical effects in small particles.

2. OPTICAL PROPERTIES OF BULK MATERIAL

Before considering deviations from bulk behavior, we need to establish the definitions for bulk optical constants, then discuss briefly how these bulk optical constants are measured and how reliable they are in terms of accuracy and precision. The following section, which we feel is necessary for clearly defining quantities used, is a summary of a more complete treatment found in the monograph with Craig Bohren[1] to which the reader is referred for more details.

2.1 Definitions

The starting point of all classical descriptions of electromagnetic effects is Maxwell's equations, supplemented by the constitutive equations which introduce the material properties of the medium into the problem. The material relations are

$$\mathbf{J}_F = \sigma \mathbf{E} \quad , \tag{1}$$

$$\mathbf{B} = \mu \mathbf{H} \quad , \tag{2}$$

$$\mathbf{P} = \epsilon_0 \chi \mathbf{E} \quad , \tag{3}$$

where σ is the conductivity, μ the permeability, and χ the electric susceptibility. $\mathbf{J}_F$ is the current density associated with "free" charges, and the other symbols have their usual meanings[1]. In this chapter we will assume that the material coefficients are independent of the fields, which restricts us to linear optical effects. Some nonlinear effects may be treated in other chapters of this book, however. We also assume that the medium is homogeneous in the sense that the fields are independent of position. For the moment only, we will consider the medium to be isotropic.

If a time dependence of $\exp(-i\omega t)$ is assumed for all fields in Maxwell's equations, where we here employ SI units, and using the constitutive relations of the form given in (1) - (3), the field equations become

$$\nabla \cdot (\in \mathbf{E}_c) = 0 \quad , \tag{4}$$

$$\nabla \times \mathbf{E}_c = i\omega\mu \mathbf{H}_c \quad , \tag{5}$$

$$\nabla \cdot \mathbf{H}_c = 0 \quad , \tag{6}$$

$$\nabla \times \mathbf{H}_c = -i\omega \in \mathbf{E}_c \quad , \tag{7}$$

where the complex permittivity is

$$\in = \in_0 (1 + \chi) + i \frac{\sigma}{\omega} \quad . \tag{8}$$

Next we consider solutions of these Maxwell's equations in the form of plane waves with electric and magnetic fields given by

$$\mathbf{E}_c = \mathbf{E}_0 \exp(i\mathbf{k}\cdot\mathbf{x} - i\omega t); \quad \mathbf{H}_c = \mathbf{H}_0 \exp(i\mathbf{k}\cdot\mathbf{x} - i\omega t) \quad , \tag{9}$$

where $\mathbf{E}_0$ and $\mathbf{H}_0$ are constant vectors and $\mathbf{k}$ is a complex propagation vector. For a

homogeneous plane wave in which planes of constant phase and planes of constant amplitude coincide, $\mathbf{k} = (k' + ik'')\mathbf{e}$, where $\mathbf{e}$ is a unit vector in the direction of propagation. Then

$$k = k' + ik'' = \frac{\omega N}{c} \quad , \tag{10}$$

where c is the speed of light in vacuoo and the complex refractive index is related to the complex permittivity by

$$N = c\sqrt{\epsilon\mu} = \sqrt{\frac{\epsilon\mu}{\epsilon_0\mu_0}} = n + ik \quad . \tag{11}$$

The meaning of the real and imaginary parts of the refractive index are made clear by writing the wave equation for E as

$$E_c = E_0 \exp\left(- \frac{2\pi kz}{\lambda} \right) \exp\left(\frac{i2\pi nz}{\lambda} - i\omega t \right) \quad . \tag{12}$$

The imaginary part k determines the attenuation of the wave and the real part n determines the wavelength in the medium.

It is almost always a good approximation at any optical frequencies to assume $\mu = \mu_0$, since magnetic response cannot usually follow the rapid oscillation of the fields. With this assumption, one can relate the complex index of refraction $N = n + ik$ to the complex dielectric function (or relative permittivity) $\epsilon = \epsilon' + i\epsilon''$, as follows:

$$\epsilon' = \frac{\epsilon'}{\epsilon_0} = n^2 - k^2 \quad , \tag{13}$$

$$\epsilon'' = \frac{\epsilon''}{\epsilon_0} = 2nk \quad . \tag{14}$$

These two sets of quantities are, of course, not independent. They are both known as optical constants.

Other commonly used forms of the complex refractive index are $n' + in''$ and $\kappa n(1 + i\kappa)$. In comparing different compilations of optical constants, one should note

that in the latter expression, κ is different from k by a factor of n. The notation is common in the German literature. The + sign is a consequence of using $\exp(-i\omega t)$ as the time dependence. If $\exp(i\omega t)$ were chosen, indices of refraction would be $n - ik$, $n' - in''$, or $n(1-i\kappa)$. Fortunately the refractive indices and the dielectric functions are independent of the system of units used, although Maxwell's equations for the fields vary slightly with the system chosen.

For simplicity we have assumed isotropic material constants to this point; however, anisotropic solids may be characterized in similar fashion with the exception of the use of a tensor dielectric function. The tensor is often symmetric so that a coordinate system can be found in which it is diagonal:

$$\begin{pmatrix} \epsilon_1' + i\epsilon''_1 & 0 & 0 \\ 0 & \epsilon_2' + i\epsilon_2'' & 0 \\ 0 & 0 & \epsilon_3' + i\epsilon_3'' \end{pmatrix}$$

where ϵ_1, ϵ_2, and ϵ_3 are the principal dielectric functions. Thus if the electric field is aligned along one of the principal axes of a crystal, **P** and **E** are parallel. By suitably orienting a crystal and making measurements with polarized light, it is possible to separate the three dielectric functions and, hence, the three sets of concomitant refractive indices. For the two lowest symmetry classes of crystals (triclinic and monoclinic), the real and imaginary parts of the dielectric tensor have different principal axes, leading to all sorts of grief and horror in dealing with them.

With this necessary but perhaps boring overview of electromagnetic theory to establish our definitions, we can now proceed to the subject of how and how well these optical constants are customarily measured.

2.2 Optical Constants Measurements

The problem of where to find measured optical constants is one which has often plagued those workers who needed more than just the real index of refraction for non-absorbing materials, and required more of a wavelength range than the near visible. Primary experimental data is found scattered through a broad collection of journals. When found, the wavelength range is often too restrictive or inappropriate, and a compilation must be put together based on various authors whose numbers do not agree, necessitating value judgements on the part of the user. The situation has become a little better in recent years with the appearance of wide-ranging

compilations by Weaver et al.[2] for metals and the handbook edited by Palik[3]. Although the latter volume serves a rather special interest group in its choice of solids, the articles by a collection of authors provide an excellent summary of the methods used to determine optical constants, compilations of optical constants, and assessments of how reliable one might expect optical constants to be. One of the purposes of the present article is to point out reasons for disagreement between bulk and small-particle optical properties. One reason is simply that the reported bulk optical constants may be wrong.

One might well ask, what is so difficult about optical constants measurements? Haven't indices of refraction been reported with five-digit accuracy for the last 100 years? Yes, but only in wavelength regions where the material is transparent, and primarily in the visible region. When one deals with remote wavelength regions such as far inrared or vacuum ultraviolet, and when the material is highly absorbing, as it frequently is, two-figure accuracy is often quite good. The following brief survey of methods for determining optical constants is intended to give a better appreciation of the difficulties and the level of uncertainties involved.

Since optical constants are comprised of two numbers, it requires two or more measurements to determine both of them. These might be a transmission and a reflection measurement, two reflectance measurements at different angles or with different polarizations, etc. Solids also occur in two different types -- conductors (metals) and nonconductors (insulators and semiconductors). For insulators there is a gap between strong absorption regions due to electronic excitation, typically in the ultraviolet, and due to vibrational excitation in the infrared. The transparency of the intermediate region is disturbed mainly by impurities and imperfections[4]. In this transparent region, optical constants can be obtained from a combination of transmittance and reflectance. The undergraduate physics experiment of measuring minimum deviation in a prism of the material will accurately determine n (easily to four figures). A transmission measurement then easily determines k. In spectral regions where the solid becomes opaque, one must either prepare suitably thin specimens (perhaps thin films) or change to reflection techniques. Using reflectometry, one can either make two different reflectance measurements or measure near-normal incidence reflectance (for example) over a broad wavelength range and use Kramers-Kronig analysis[5,6] assuming suitable extrapolations of the measurements to zero and to infinity. Ellipsometry may also be employed[7], in which amplitude ratios and phase shifts are determined.

2.3 Difficulties and Uncertainties

Each of these techniques for determining optical constants has its strong and its weak points (see Refs. 2 and 3). Transmission measurements are easy and accurate, but thin films required in strongly absorbing regions may not be producible in bulk crystalline form. The use of Kramers-Kronig analysis of single reflectance measurements as a function of wavelength is convenient to do in the vacuum ultraviolet, but the extrapolation problem can be severe. Ellipsometry overcomes many of these problems but is difficult in the far ultraviolet and far infrared because quality polarizing components required may not be available.

Difficulties in determining optical constants can generally be divided into two categories -- instrumentation problems and sample preparation difficulties. In the photometry, experimental problems include light source stability, stray light and higher-order grating effects in monochromators, and detector nonlinearity and nonhomogeneity. In ellipsometry, one has sensitivity to alignment of polarizing elements, imperfections in these optical elements, and sensitivity of detectors to polarization. In the preparation of samples, various problems cause difficulty because of the need to produce clean, flat, strain-free surfaces that are representative of the bulk material that is to be measured. Some of the difficult problems with achieving this ideal sample configuration for photometry and ellipsometry are the following:

1. Surface contamination -- adsorbed films and oxide layers on metals.
2. Rough surfaces.
3. Amorphous surface layers on crystals -- produced by cutting and polishing operations.
4. Strained and damaged surface layers.
5. Porous material which affects bulk density -- common in evaporated films.

Because of all these problems, highly accurate optical constants are rarely available for a given material, and tabulated values are seldom as accurate as the number of significant figures cited might suggest. The volume edited by Palik[3], where individual authors write about their favorite techniques and cooperate to give critical evaluations of optical constants for certain solids, gives an excellent overview of the situation. Because of the struggle of these authors to reconcile n's and k's from various sources, their advice on how good the resulting values are consitutes a valuable summary. We quote their words. "Unfortunately the variations in n and k

are such that for nontransmission experiments generally, only one or two figures should be used in quoting absolute values (accuracy), while more are often carried along to show spectral structure as a function of wavelength (precision). Only in the case of measurement of refractive index by minimum deviation or fringes are we able to set down values to four decimal places with some confidence. While we can give examples of ellipsometric measurements and KK analysis of reflectivity in an overlap region (1.5 to 6.0 eV) that agrees to two figures, we also have examples in which two laboratories measuring R and doing KK analysis hardly agree to two figures among themselves."[8]. In discussing "use and misuse" of their critically compiled results for metals, Weaver et al.[9] state, "We believe that the data tabulated are good to within + or - 10% in most cases ... . The potential user should keep this 10% figure in mind for critical applications." To this we add Amen. And if teams of critical experts, many of whom have made their reputations on such measurements, claim these sorts of uncertainties, how inaccurate should one presume are measurements reported by only one worker? Factor-of-two discrepancies are not unusual in the two compilations just referred to, even among reputable workers. In certain difficult situations, order-of-magnitude disagreements are prevalent. For example, in the difficult case of graphite oriented with its easy cleavage planes perpendicular to the electric field direction, even the qualitative nature of the optical constants is in dispute[10]. As Aspnes has concluded[11], "The problem of accurate determination of intrinsic dielectric properties has not yet been solved in general."

3. OPTICAL PROPERTIES OF SMALL PARTICLES

Before going on to discuss some deviations from bulk n and k that have been observed or calculated to occur, we want to make one point clearly -- optical properties of small particles may be quite different from bulk samples without any breakdown of optical constants. However, since intuition may not be a safe guide as to how small particles should behave, one may have to calculate the optical properties using small-particle theories such as the so-called Rayleigh theory or the Mie theory. When this is done, the particulate optical properties emerge.

3.1 Calculated Optical Properties

Perhaps the most long-standing example of varying optical properties in a small-particle system is the color variation of colloidal metal particles, whose understanding was in fact the stimulus for the theoretical work of Gustav Mie[12]. In attempting to understand the colors of colloidal gold in water, Mie provided one of the early solutions to the problem of interaction of a plane electromagnetic wave with a sphere of arbitrary size characterized by bulk optical constants. The name of Mie is a nice, concise way of referring to this classic solution; for some history on others who perhaps should share the glory, the reader may note the comments in Kerker's book[13]. Even without the use of computers, Mie was able to explain the vivid colors of the gold colloids which had in fact been under observation for centuries in some of the colors of stained glass prepared with embedded metal particles[14].

A calculated example using Mie theory is shown in Figure 2, where the extinction per unit volume of metal is shown for several radii of single spheres of aluminum. (Extinction in small-particle optics refers to the attenuation of light by both loss mechanisms, scattering, and absorption.) Optical constants used as input were taken from the measurements of Hagemann et al.[15] fitted to a Drude theory. Note first the dominant peak in extinction near 8 eV which does not correspond to any feature in the bulk optical constants. The peak is due to a very strong interaction of light with the free conduction electrons of the aluminum. As the electrons collectively slosh back and forth in the particle, they are confined by the surfaces, producing large depolarization effects which cause the electron cloud to resonate at a quite different frequency than it would in the absence of the confining sphere. The absorption is usually referred to as the surface plasmon resonance, although this term is somewhat of a misnomer for the smallest particles[16].

Since the Mie theory casts the solution of the sphere problem in infinite series of terms that effectively mask what is happening, it is convenient and very useful to introduce the Rayleigh approximation for a single sphere[17]. Although extinction is the easier to treat theoretically, the difference between absorption and extinction becomes vanishingly small in the small size limit of Rayleigh theory. The approximation is valid in the limit of small radius ($x << 1$) and in the limit of zero phase shift in the particle ($|m|x << 1$), where m is the relative (complex) refractive index of the sphere with respect to the host medium and $x = 2\pi a/\lambda$. In this limit extinction for a sphere in vacuum, normalized per unit volume of material is

$$\alpha = \frac{6\pi}{\lambda} \operatorname{Im}\left\{\frac{\epsilon-1}{\epsilon+2}\right\} \quad . \tag{15}$$

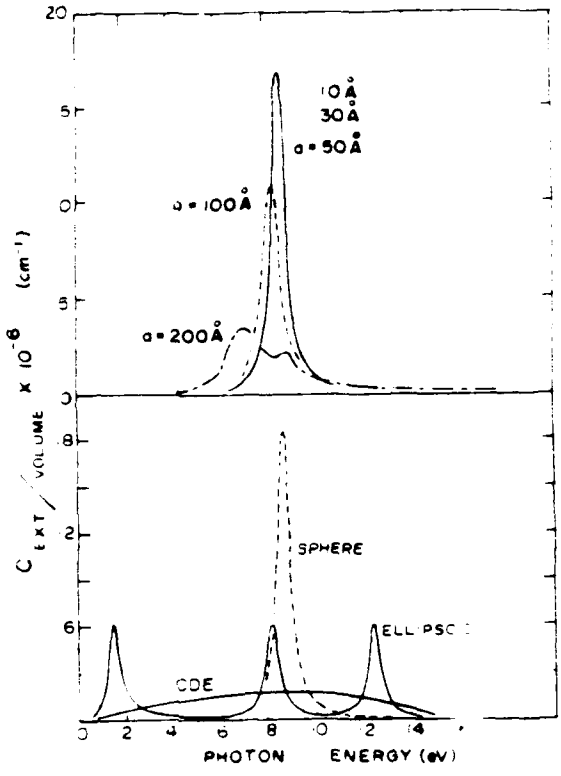

Figure 2. Calculated extinction cross sections normalized per unit volume for spheres of aluminum using Mie theory (upper curves and lower dashed curve) and for a single ellipsoid and a continuous distribution of ellipsoidal shapes (CDE) in the Rayleigh approximation (lower curves).

It is quite obvious that whenever $\epsilon = -2$, there is a pole in the extinction efficiency. This is the "magic number" for dielectric functions as concerns small-particle properties. Although this condition does not occur in any common solid or liquid in the visible, it is a very common condition for metals in the ultraviolet and for various insulating solids in the infrared.

Returning now to the calculated optical properties of small aluminum particles in Figure 2, we note that below about 50 Å, all curves are exactly the same and are

shown as one. There is no change in absorption spectrum with size. This is an important point, since any real deviations in position or shape of the peak can only be due to deviations in bulk optical constants. The conditions of the particle being a smooth, homogeneous sphere should be clearly kept in mind, however.

Nonspherical shapes also produce strong effects on surface-mode absorption. In general, absorption by nonspherical shapes is difficult to calculate, but the Rayleigh approximation is simple enough to give closed-form expressions for an ellipsoid which can then be conveniently taken to its limiting shapes. Expressions for extinction by an ellipsoid in the Rayleigh approximation, both oriented and randomly oriented, are given[17] in Chapter 5 of Ref. 1. The calculated effect of ellipsoidal shape on the surface plasmon absorption in aluminum is shown in the bottom part of Figure 2. When averaged over all orientations of the ellipsoid with respect to the incident electric vector, there appear three peaks corresponding to the three shape factors of the ellipsoid. Depending on the extent of the stretching or squashing of the ellipsoid, the resonances can occur quite far from the sphere resonance, but always confined to the negative ϵ' region. It is thus clear that a distribution of shapes modeled by varied ellipsoidal shape parameters could give rise to a broadening of the plasma resonance peak. To illustrate an extreme but useful approximation, we also show in Figure 2 a simple calculation of a continuous distribution of ellipsoidal shapes in the Rayleigh approximation[18], using the same bulk optical constants of aluminum.

Summarizing the important optical effects of small particles calculable from bulk optical contants, we repeat that small particles can show quite different optical absorption spectra than the parent material. The most extreme variations occur in the vicinity of surface mode resonances, characteristically in the UV for metals and in the infrared for insulators. In the small size limit, these resonances are size independent, leading to the possibility of recognizing non-bulk effects by observing deviations from the small size limit. Unfortunately, nonspherical shape effects, for example, also produce strong deviations from the limiting sphere behavior just in these regions.

3.2 Apparent Deviations from Bulk Behavior Because of Clumping

From a calculational point of view, it is easy these days to compute any optical properties of distributions of homogeneous spheres. With more effort, the same can be done for spheroids and for infinitely long cylinders, which give good approximations to very long, finite cylinders. The irregular and randomly distributed

shapes which frequently (usually) characterize collections of small particles are very difficult to treat. An even greater difficulty is to deal with the almost inevitable clumping of particles when dealing with collections of particles. On the experimental side, the big difficulty is in producing isolated particles — that is, particles that do not occur as clumped aggregates. The problem of isolating particles is a huge problem. Failure to make the experimental system obey the independent particle criterion has led to numerous, serious errors in comparing measurements with theory. Examples are covered in the next paragraph, followed by a brief discussion of ways in which isolation of particles is being achieved.

During the years from about 1960, there began to be considerable interest in the infrared properties of ionic crystals in small-particle form. In an ionic crystal, the electromagnetic wave couples to the long-wavelength optical phonon mode (out of all the many vibrational modes present in the crystal) in order to conserve momentum and energy between the absorbed photon and the emitted phonon. Because of this strong coupling predominantly to one mode, the oscillator strength of the transition is very large, giving rise to a very strong absorption band with attendant large swings in the optical constants. The resultant strong swings in polarizability of the crystal under the action of the electromagnetic wave give rise to important depolarization effects at the boundaries of small particles. Thus the dominant absorption band peaks at a quite different energy in a small ionic crystal sphere than in a bulk slab of the same material. Nonspherical shape effects are also significant in these cases, although they are much harder to calculate. In most of the early work which is surveyed in Refs. 19 and 20, experiments were done on particles collected on infrared-transparent substrates or dispersed by mixing with a powder of transparent material (such as KBr) and pressing a disc for infrared transmission studies. Resulting spectra were almost invariably compared with spherical small-particle calculations. Although peak positions agreed fairly well between measurements and calculations, peak widths were extremely different. Measured absorption peak widths were sometimes an order of magnitude greater than those calculated using bulk optical constants. There was an initial tendency to explain the discrepancy as due to a breakdown of the bulk optical constants, which in the case of some powders must have happened in particles of micron size, predominantly. Quantum size effects were hopefully discussed. Later work has shown that the almost unavoidable clumping of individual particles to produce effective particles of very complex shape is the reason for the poor agreement with isolated sphere calculations.

A clear illustration of the effect of clumping is given by work on infrared absorption by silica (amorphous SiO_2). Although it is frequently difficult to make perfectly spherical particles of most solids, the particles from silica smoke are perfect spheres — as accurately as we can determine from electron micrographs. These particles are easily produced by striking an arc in air between silicon electrodes. The resultant smoke consists of spheres with diameters ranging from about 100 Å to about 1000 Å. In addition to being spherical, they have the desirable characteristics of being isotropic, composed of material with accurately measured infrared optical constants, and the size is well within the range where volumetric absorption is independent of size. In our first published measurements of infrared extinction[21], we found a discrepancy of about a factor of 2.2 between measurements and calculations. In subsequent work[22] it was proven that trying harder to break up the clusters of spheres decreased the discrepancy markedly. After mixing the small sample of weighed silica into the KBr matrix powder, the usual agitation in a dental amalgomator was extended from minutes to hours to days to weeks. The height of the volume-normalized extinction peak steadily increased with agitation times up to about a week. Figure 3 shows the results of comparing measurements on our most well-dispersed samples with calculations of the same quantity based on bulk optical constants. Also shown are the previously published results of the peak extinction obtained after normal short-time dispersal. The remaining discrepancy at the peak is about 20%. The additional broadening in the wings of the peak leads us to believe that residual clumping is still degrading the experimental results with respect to the calculations. Nevertheless, the remaining disagreement is now small enough to suggest that there is no large change in bulk optical constants for particles of this size, especially in view of possible uncertainties in bulk optical constants measurements pointed out in Section 2.

Another example of previously published work which clearly shows the effect of agglomeration is our results on similar dispersal experiments of MgO in KBr matrices[23]. Smoke particles of MgO are readily produced by burning magnesium ribbon in air. In this case the particles are very perfect cubes, as shown by electron micrographs. First the particles were simply collected on the substrate. Successive levels of dispersal were then produced by shaking the KBr-sample mixture in a glass vial with steel balls, first for the usual few minutes, then for 3 hours and then 3 days. Transmission spectroscopy on KBr discs pressed from these dispersions produced steadily evolving infrared spectra. Various calculations were compared with the

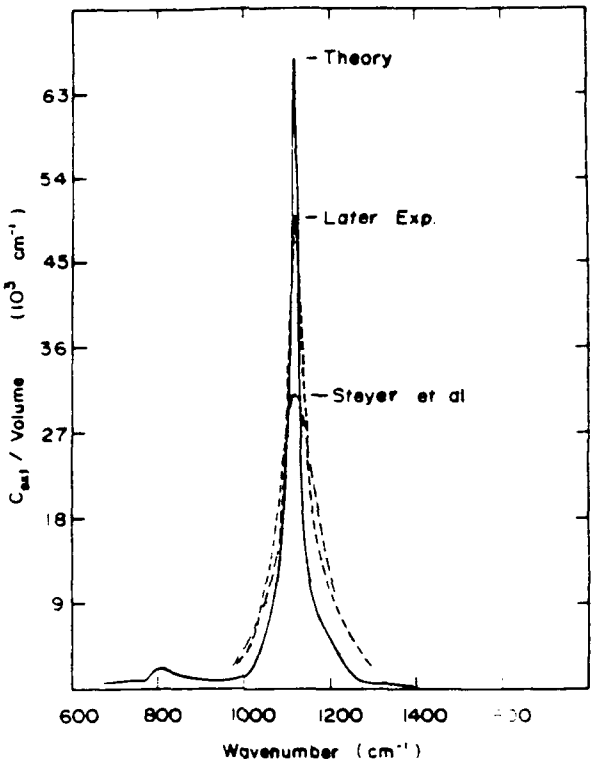

Figure 3. Volume-normalized extinction for fused quartz smoke particles measured by the KBr pettle technique (dashed lines) and calculated (solid line) assuming spheres and measured bulk optical constants. The lower dashed curve is taken from the older measurements of Steyer et al.[21].

measurements. Sphere calculations compared poorly with all measurements. The simple calculations based on a continuous distribution of ellipsoidal shapes in the Rayleigh limit (CDE) gave a better approximation to the messy tangle of particles on the surface. Succesively more effective dispersal showed an approach toward a Rayleigh calculation for cubes done by Fuchs[24], using bulk optical constants. Even the splitting of the two most prominent cube modes was revealed by more dispersal.

Another case in which particle aggregation plays an important, if not the sole, role in disagreements between measured extinction by small particles and calculations is that of the far-infrared absorption by metal particles such as aluminum. This situation will be discussed in Section 4.4.

It is now clear that aggregation of particles is a major problem. While we may like to imagine our particles as the little separate entities assumed in most of our calculations, glances at almost any electron micrograph of particulate samples shows a very different real life picture -- clumps of particles.

3.3 Methods of Studying Isolated Particles

Having finally realized the seriousness of the aggregation problem in our own experimental program, we began to think long and hard about how we could get around it. The vigorous dispersion in KBr worked to some extent, but only at the expense of considerable effort and the possibility of unwanted damage to the particles in the process. It seemed that one viable approach would be to create the particles in a separated state and not allow them to get together until measurements are completed. Another idea was to make the measurements quickly, before the rapid coalescence could take place. A third (far out) idea was to examine particles in remote regions where they may not have had the opportunity to clump, such as in interstellar space. In fact, we, along with many others, have explored all of these avenues to some extent. Some of the results are discussed in Section 5.

A listing of some of the techniques that have been used to produce isolated small-particle samples for optical study is given below. References are intended only to show the interested reader a direction or two in which to go in order to pursue the techniques.

1. Low temperature matrix isolation in solid rare gases, with annealing for controlled growth[25,26].
2. Arrested growth of colloids[27].
3. In-situ measurements of gas phase aggregation[28,29].
4. Growth of metals in photosensitive glasses[30,31].
5. Aggregated color centers in alkali halide crystals[32].
6. KBr pellet dispersal for infrared spectroscopy, discussed above.

4. DEVIATIONS FROM BULK OPTICAL BEHAVIOR

Although we previously stated that small particles at some size obviously suffer a breakdown of bulk optical properties, we have spent some time showing the difficulty of discovering such effects. In this section, however, we present results that clearly show the inadequacy of bulk optical constants, first in the case of molecular clusters with different crystal structure from the bulk, next for quantum size effects in non-conductors, and finally in the case of metals. In the latter case, the argument for quantum size effects is weaker. In the case of anamolous far-infrared absorption in metal particles, there is hardly a case for quantum size effects from the experimental data.

4.1 Changing Crystal Structure

During the growth of microcrystals starting from atoms or molecules, a variety of symmetries occur. Because of recent interest in cluster physics, several groups have treated extensively the structure and stability of small clusters. Figure 4 illustrates the configuration of atoms in the lowest energy arrangement deduced from calculations on silicon[33], carbon[34], and sodium chloride[35]. One of the most interesting questions associated with this kind of work is whether or not the small clusters can be considered to be small pieces of bulk crystal and, if not, to what size must the clusters grow before becoming microcrystals of bulk material? For example, in the diamond structure characteristic of bulk crystalline silicon, one might expect four silicon atoms (Si_4) to have a tetrahedral and Si_5 to form a pyramidal structure. The figure shows, however, that small clusters of silicon are all different from pieces of bulk crystal in the sizes shown. This is apparently due to the many dangling bonds inherent in small pieces of the crystal which act like a surface tension, driving the clusters toward more compact geometries[33]. On the basis of this concept, Tomanek and Schlüter[36] have estimated the transition to bulk structure to occur for clusters of several hundred atoms.

Small carbon clusters appear to be quite varied with linear structures alternating with cyclic structures. As the size increases to greater than 10 atoms, the cyclic form appears to be favored, although dangling bonds on the perimeter may prevent graphite-like layers from forming until much larger clusters occur. At a size of 60 carbon atoms, there appears to be a very stable "magic number" cluster consisting of carbon atoms at each vertex of a soccer ball geometry. Stability near

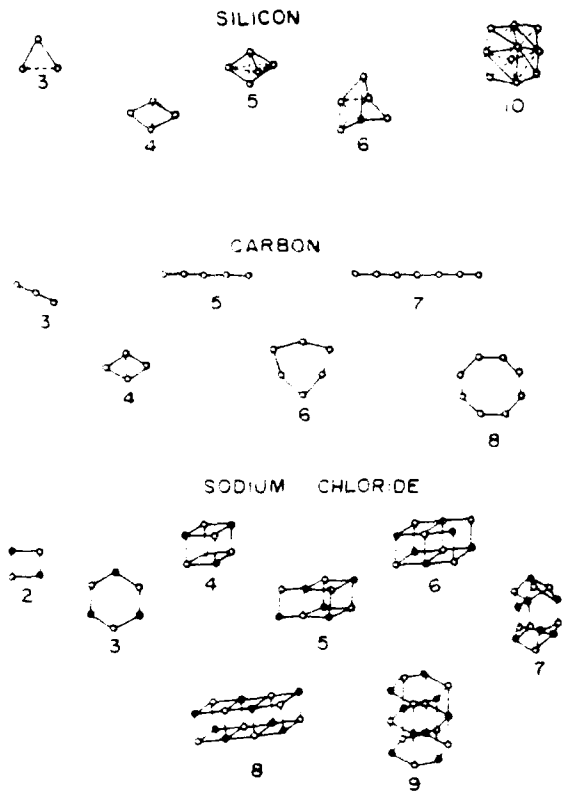

Figure 4. Calculated cluster geometries for some small clusters of silicon and carbon atoms, from Brown et al.[33] and for small clusters of sodium chloride molecules, from Martin[35].

because there are no dangling bonds. There is even speculation[38] that this highly stable structure forms a nucleation site for small-particle growth leading to common soot particles, which commonly occur as spheres with a complicated radial layering[39].

Extensive calculations of stable configurations in clusters of alkali halide molecules have been made by T. P. Martin[35], from which the predicted configurations of $(NaCl)_n$ in Figure 4 are taken. The calculations predict that the four atom dimer $(NaCl)_2$ forms a rectangle, but the trimer prefers a six-atom ring over a rectangular plane. Both the dimer, which looks like it belongs to a NaCl-type lattice and the trimer, which doesn't, form two kinds of building blocks which fit into the cubic scheme. As in the figure, the clusters of molecules built from dimer units approximate a piece of the bulk structure, while the $(NaCl)_9$ cluster built from trimers

is quite different. As Martin concludes, "clearly, for smaller clusters, structures resembling a portion of an NaCl lattice are not always energetically favored."

It is clear that at least some of the structures pictured in Figure 4 would have optical properties that could not be predicted from bulk optical constants for two reasons — the atomic arrangement characteristic of the bulk has not yet developed, and there is a preponderance of surface atoms not found in great abundance in the bulk.

The natural occurrence in our environment of small clusters of molecules is rare. Although such clusters must occur in the early growth stages of small particles, great effort and cleverness is usually required to arrest the growth at a particular cluster size. Despite the rarity of these small entities, their structure may be quite important in determining structural properties of much larger particles, perhaps enforcing on the particles a structure that would be quite uncommon in bulk matter.

For a number of years we have been intrigued by the properties of iron oxide smoke produced, for example, by arc electrodes of iron burning in air. The particles are characteristically a few hundred angstroms in size and invariably have the cubic crystalline form of γ-Fe_2O_3. In the bulk, this form goes over irreversibly into the stable α-Fe_2O_3 (hematite) form. Because of the temperature instability of the bulk γ form, it has not been possible to produce bulk single crystals, which thereby prevents us from measuring bulk optical constants for the small-particle form. A similar behavior occurs in the production of very small particle Al_2O_3, which also prefers the cubic form over the stable bulk form of α-Al_2O_3.

If we imagine the nucleation and growth of particles of, let's say, 100 Å and greater in size from initial clusters of varying structure, as surveyed in Figure 4, perhaps it is not surprising that many small-particle systems seem to have structures that are different from the corresponding bulk crystals. This may also help to explain why many small particles often grow in a very confused way, leading to highly disordered or amorphous structures. Examples of the prevalence and importance of such disordered structures in small-particle systems are given in Section 5.

4.2 Quantum Size Effects in Non-Conductors

Solids generally can be divided into two distinctly different classes optically -- metals (or conductors) whose free electrons absorb all frequencies, and non-metals, which have forbidden gaps of varying energy between occupied and unoccupied

electron energy bands. Even when the cluster size is large enough for bulk lattice structure to dominate, it is possible for small-particle deviations to occur. These are generally called quantum size effects (QSE's).

In a recent article, Brus[40] has surveyed the evidence for non-bulk-like behavior in semiconductor clusters which have bulk-like crystal structure. Most of this work at Bell Labs[41] has been done on sulfides and selenides of Zn, Cd, Pb, etc., because of the comparative ease of sample preparation, although Brus gives references to reports of quantum size effects in other semiconductors. In general, crystallites of the order of 100 Å in diameter show optical absorption that is identical with bulk crystal absorption, at least at low spectral resolution. In microcrystals of 40-50 Å, the absorption edge begins to show a blue shift (to higher energies), and at 20-30 Å diameter, the absorption edge has shifted more than one electron volt. The reason for the rather slow convergence to bulk optical properties with increasing size lies in the strong directional bonding in these materials, which dominates the band-gap region.

In similar work in Berlin on colloidal CdS[42] and ZnS[43], the authors found structure in the absorption spectrum related to the size of the clusters. The smaller clusters occur in multiples of certain discrete sizes. Absorption spectra of the different sizes show discrete peaks in the absorption edge which the authors relate to different numbers of the basic unit. Further, the absorption edge shifts toward shorter wavelengths, as in the work of the Bell Labs group, as size decreases until "yellow" CdS becomes colorless when the absorption edge has moved entirely into the UV. It seems clear that in these cases there is a size dependence of optical properties that is not predictable using bulk optical constants in Rayleigh theory, including any shapes. The German workers have even coined a new term "Q-state," where they explain that "Q stands for unusual quantum effects that lead to different physical or chemical properties of a material as compared to those of macropieces of the material"[44]. Inspiration for designation of yet another new state of matter appears to come from W. Ostwald's book, "Die Welt der nernachlässigten Dimensionen (The World of the Neglected Dimension)"[45].

4.3 Possible Quantum Effects on Surface Plasmons

Since the surface plasmon band so thoroughly dominates the optical properties of small metal particles (see Figure 2, for example), many experiments have been done to investigate the characteristics of the band as a function of particle size. It is

fortunate from the standpoint of being able to identify changes from bulk behavior that changes in the surface plasmon band for spherical particles can only be due to deviations from bulk behavior. Two principal effects may occur as a function of size — a shift of the band and a change in the width. Both theoretical and experimental results on the subject have been recently reviewed by Kreibig and Genzel[46], two authors who have been active in this field for many years. As far as surface plasmon peak shifts go, their conclusion is that the shift is too small and can originate from too many different causes to enable any conclusions to be drawn from the measurements.

Both quantum-mechanical[47-50] and classical models[51-53] (see Ref. 46 for a more complete listing) have been used to explain changes in the surface plasmon band as the size decreases. The basic idea of the classical model is simply that the damping constant in the Drude free-electron theory, which is the inverse of the collision time for conduction electrons, is increased because of increased collisions with the boundary of the particle. Assuming that the electrons are diffusly reflected at the boundaries, the damping constant γ can be written

$$\gamma = \gamma_{bulk} + A \frac{v_F}{a} ,$$

where γ_{bulk} is the bulk metal damping constant, v_F is the free-electron velocity at the Fermi surface, and A is a constant, empirically found to be of order unity. Although classical limitation of the mean-free path has a small effect on peak position, it has a marked effect on peak width.

In an oft-quoted paper, Kawabata and Kubo[47] have argued that the classical description is inadequate in the sense that the energy spectrum is discrete, with the spacing increasing as the particle size decreases. The width of the resonance should be described then as due to the plasma mode damping due to excitation of one-particle modes. Although the quantum mechanical treatment would appear to be the correct approach, the peak width measured experimentally has consistently shown better agreement with the classical theory of limitation of mean-free paths. The A parameter seems to be quite sensitive to the assumed nature of the electron density profile at the surface[46]. Because of this sensitivity, the parameter may be well-suited to explore both size effects and interface effects. There is also a rather strong dependence of the A parameter on the embedding material, which is not simple to explain. The present state of the classical vs. quantum-mechanical controversy seems

to be that the classical theory consistently gives better agreement with experiment. There is, however, recent work[54,55] on silver particles isolated in rare gas matrices which shows narrower peaks than previously measured. These appear to be more consistent with the Kawabata and Kubo theory. We should also note that nonspherical shape distributions clearly give rise to broadening of the surface plasmon peak, as shown in Section 3.2 and Figure 2. In view of the experimental difficulties of producing perfectly isolated spherical particles, we must always remain aware that measured shifts and broadenings may still be more affected by these nonidealities than by the quantum level spacing or the mean-free paths.

Although there is still room for debate on whether quantum size effects have been observed in the surface plasmon bands of metal particles[46,56], both sides agree that there are effects taking place that cause modification of the bulk optical constants.

4.4 Far-Infrared Absorption in Metals

As emphasized by Kawabata and Kubo[47], as well as Gor'kov and Eliashberg[50], quantum level spacing should occur in small particles. The expected region for observation would be the far infrared, where the energy-level differences would more nearly correspond to photon energies. Early reports of structure[57] that might be due to quantum level spacing were not confirmed by more careful subsequent work[58]; however, an increased absorption in the far infrared amounting to about three orders of magnitude was observed over predictions of either the Gor'kov-Eliashberg theory or the classical Drude theory. The failure to see structure caused by quantum effects was understandable, since any reasonable size distribution would wash out the peaks[59]. The enhanced absorption stimulated a number of theoretical explanations referred to in our Refs. 56, 60, and 61. In more recent work, care has been taken to control the degree of aggregation, with the result that, for the most well-dispersed Ag particles, the authors conclude[61], "the far-infrared absorption coefficient is enhanced by a factor of 100 at most, and the data are consistent with no enhancement whatsoever." Thus the experimentalists are again faced with the difficult old problem of eliminating clustering in order for the experiment to relate properly to the theory. Because the absorption coefficients for metal particles in the far infrared are so low, the requirement of separating the particles from one another and providing enough total absorption to measure with certainty demands rather long path lengths that will be difficult to achieve in common isolation techniques such as

low-temperature matrix isolation or gas-phase isolation. Perhaps we must wait until we can effectively do experiments in the clean environment of space, earth orbit or beyond, where long path lengths should present no problem, in order to totally isolate the metal particles for doing far-infrared spectroscopy. Perhaps then, the clumping effects can be minimized to the point where we can hope to see other, more interesting effects. Until improved experiments are done, we have no really convincing evidence for quantum size effects in the far-infrared spectrum.

5. SOME EXAMPLES

In order to exemplify various camparisons of small-particle measurements with calculations based on bulk optical constants, we have chosen to discuss measurements of graphitic carbon, the insulating silicate mineral olivine, and metallic silver. Since most of the work reported here is from our own laboratory, we will not hesitate to be rather personal in reporting it.

5.1 Carbon

Carbon is a ubiquitious, cosmic solid that is important in several areas of applied, small-particle physics. In the earth's atmosphere, it is probably the dominant absorbing component of the aerosol[62]. As such, it affects the earth's heat balance and the trend of global temperatures. In the recent flurry of activity over nuclear-winter scenarios, carbon is an important component[63]. Cosmically, carbon is by far the dominant element which forms stable solids. Now considered to be an important component of interstellar dust, it is thought to give rise to the 2200 Å band observed almost everywhere in interstellar dust[10]. Recently, clusters of carbon atoms are being considered seriously to explain long unidentified interstellar absorption bands[64], as well as unidentified emission bands in the infrared[65-66].

Pure carbon occurs in several allotropic forms, including the distinctly different graphite and diamond. Graphite is a highly anisotropic, uniaxial crystal whose properties along the unique c-axis are totally different from optical properties with the electric vector oriented normal to the unique axis. Because of the ease of cleavage along planes perpendicular to the c-axis to produce atomically smooth and clean surfaces, the optical constants for electric fields perpendicular to c are more accurate and reliable of the two. Even for this "easy" orientation, there may be substantial

difficulties with published values of n and k[10]. In the far infrared, the reflectance approaches 100%. Small deviations from 100% result in very large changes in optical constants. Sato[67] reported a dip amounting to a few percent near 80 μm, which gave rise to swings in optical constants amounting to more than an order of magnitude. Later, Philipp[68] accepted Sato's reflectance dip but improved the low energy extrapolation and calculated optical constants. More recent studies in our lab and at the University of Missouri at Rolla[69] indicate that there is no measurable dip in reflectance near 80 μm in room-temperature reflectance. If this is true, it would mean that the optical constants for graphite in the most readily accessible E⊥c orientation are in error, and resulting calculations of far-infrared extinction in graphite[70] are substantially in error because of this.

Although we have tried many times, we have not yet succeeded in producing and measuring small-particle extinction for graphite in the infrared with any degree of successful comparison between theory and experiment. The problem of unknown optical constants is one problem, but there are are severe experimental difficulties. It is very difficult to produce particles for measurement that are individual and isolated, and it is very difficult (perhaps impossible) to produce single-crystal particles of graphite in the 100 to 300 Å size range. Because of the difficulties in controlling particle agglomeration, we turned to experiments in which we have tried to build up clusters of atoms from a few in number to a large enough number for the particles to act as bulk crystals.

The experiments described here have been carried out in collaboration with W. Krätschmer[71]. We chose to isolate the carbon clusters formed by vaporization of graphite, in a low temperature, solid argon matrix. Annealing of the argon matrix would then allow controlled growth of clusters of carbon. Already in the vapor state, carbon is different from most monatomic solids in that three atom clusters are dominant. The yield of C_1, C_2, and C_3 is in the approximate ratios of 30% to 10% to 60%[72]. Thus, carbon has a head start in the game of producing large clusters by agglomeration of smaller ones. Optical absorption of the carbon carrying matrix is conveniently done in conventional double-beam spectrophotometers. Representative spectra are shown in Figure 5. The rich spectral structure is very repeatable from run to run. A band near 4050 Å, known to be due to C_3, is observed to decrease as other bands grow in the annealing process. At first[64], it appeared that we were observing a series of linear carbon molecules, which had been predicted to be the

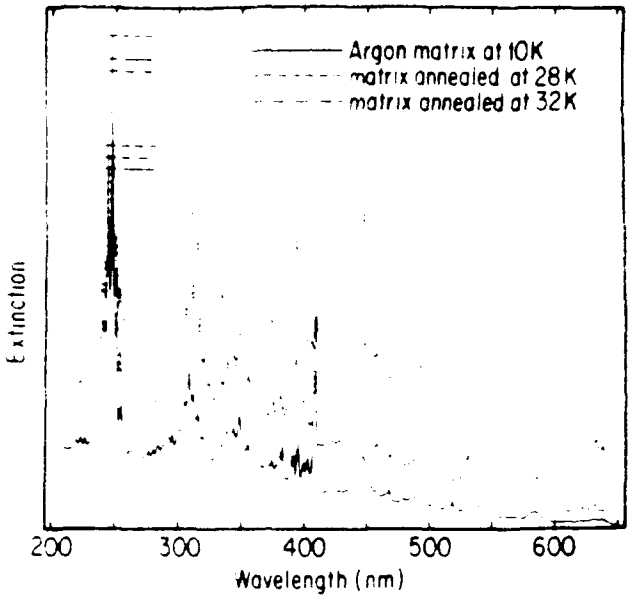

Figure 5. Absorption spectra of carbon isolated in low temperature, solid argon matrices, with increasing annealing in the upper two curves (after Kratschmer, Sorg, and Huffman[64]).

preferred configuration based on energy-level calculations[73]. If this were so, it might represent a one-dimensional particle-in-a-box whose energy-level spacing would decrease as the number of particles in the chain increases. In fact, our first identification[64], which is very likely wrong, predicted bands of increasing energy as the linear clusters increased in size from C_2 to about C_9. More recent calculations[74-75], although not in total agreement among themselves, suggest that the carbon clusters of increasing size have a more complicated series of shapes, perhaps, as shown in Figure 4. Work is continuing in an attempt to identify the various bands with specific clusters. The methods being used are correlation of growth and decay rates of individual bands in conjunction with theoretical calculations, and correlations between infrared lattice absorption bands and visible-UV electron transition bands in the same clusters. Although identification of all bands is far from complete, it is clear that the complexity of the cluster absorption grows as the sizes increase.

Graphite is usually classed as a semi-metal[39]. This is because of a very small degree of electron band overlap giving it some of the characteristics of a metal. It is, of course, highly anisotropic, with the optical properties for electric field parallel to

the c-axis resembling more those of an insulator. Although graphite is not a good metal, delocalization of π electrons within the parallel sheets of the structure give rise to a free electron type of plasma. The dielectric function for $E \perp c$ shows a dip into the negative region which, according to the previous discussion in Section 3.1, produces a shifted surface plasmon absorption peak.

Mainly because of its astrophysical interest, small graphitic carbon particles have been studied in the UV region by several authors[10,76,77]. So far there are no reports of carbon smoke studied spectroscopically in the gas-supported phase or isolated in a dilute way in a low cryogenic matrix; all the cited measurements are for carbon smoke collected on substrates. Although we cannot expect identity of these measurements with single-particle calculations in view of the difficulties discussed in Section 3.2, the surface plasmon peak shows up easily in the carbon-on-substrate method. In a more recent effort to study the 2200 Å band in the laboratory, we set up a new production chamber in the laboratory of W. Krätschmer. To our amazement, the first attempts to study the (previously) ever-present plasmon feature showed no indication of it. After a few tries using variable conditions, it was found that we could produce carbon smokes that either did or did not show the UV feature. Figure 6 shows typical absorption (extinction) spectra; the sample produced in 20 torr of helium showed the usual absorption band near 2200 Å, while the sample produced in 2 torr of helium showed no indication of it. We should also admit that other conditions, such as the shape of the electrode tips and the degree of violence in the few seconds of vaporization, played important roles in keeping the results from being totally predictable from run to run. Nevertheless, two distinct types of spectra occurred -- with the plasmon band and without. It was also noticed that very gentle heating for a few minutes on a laboratory hot plate (temperature about 200 C) sufficed to turn the "no-hump" sample into one with a proper hump. This is shown in Figure 6(b). Raman spectroscopy of the usual graphite smoke showed the two-band spectrum characteristic of disordered graphite. Single-crystal graphite shows only a single peak near 1600 cm^{-1}, while a second peak occurred in the vicinity of the approximately 1300 cm^{-1} position characteristic of single crystal diamond. The usual exlanation[78] is that the disorder introduces some diamond-like tetrahedral bonding into the graphitic small particle, giving rise to the second peak.

The Raman spectrum of our sample which showed no surface plasmon peak is shown in Figure 7, both before and after the gentle heating. Although the post-heating sample has a Raman spectrum which is very similar to the usual carbon

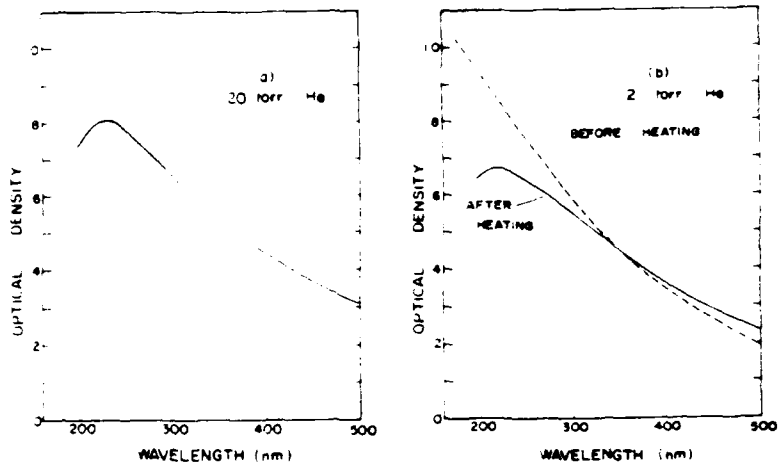

Figure 6. Extinction spectra for smoke from gaphite electrodes collected on quartz substrates, for two different pressures of He gas in the production chamber. For the 2 torr sample, spectra are shown before and after heating to about 200 C for a few minutes in air.

smoke sample, the "no-hump" sample shows no sign of the characteristic double-peaked Raman spectrum. In fact, the single broad peak near 1500 cm^{-1} is almost identical in shape to a Raman spectrum of graphite which had been subjected to a very heavy dose of damaging bombardment from high energy, heavy ions[79]. With this in mind, it seems clear that our "no-hump" sample consists of such highly disordered small particles of carbon that there is too little of a free-electron nature to the π electrons to permit a measureable surface plasmon band to form. What was surprising to us was that such a small amount of heating could make such a large change in urging the structure in the direction of a graphitic structure in such a high temperature material as graphitic carbon. The highly disordered phase can perhaps be thought of as the result of the complex collection of pre-particle clusters that go into making up the small particles. Once formed, however, these small particles are on the verge of instability, seeming to desire just a little encouragement to move toward more of a crystalline nature. It goes without saying that the no-hump carbon particles would be very poorly modeled using optical constants of the bulk graphite from which they were vaporized and reconstituted.

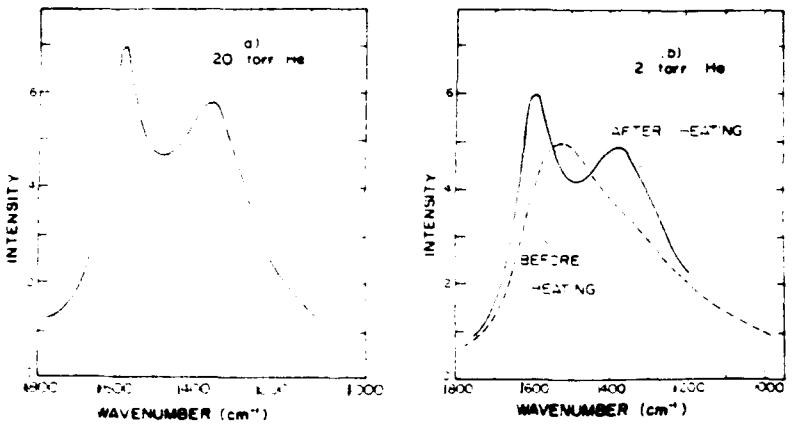

Figure 7. Raman spectra for the two smoke samples from gaphite electrodes for which extinction is shown in Figure 6.

5.2 Olivine

Olivine is the mineral name for the magnesium-iron silicate with the composition $(Mg,Fe)_2SiO_4$. In the early 1970's we began work on both the optical constants of bulk olivine and the small-particle extinction characteristics. Olivine had been calculated to be one of the dominant small-particle condensates in the atmospheres of cool stars[80], a supposed source of interstellar dust. Since a strong circumstellar emission feature near 10 μm wavelength seemed to be a signature of Si-O stretching-mode vibrations, it was important to this subfield of astrophysics to have good optical constants for olivine for the purpose of modeling absorption, scattering, and emission from tiny particles of such material. Unfortunately for the measurers, the olivine crystal structure has three principal axes. The good news was that the three axes were at least orthogonal, so that three different sets of measurements on oriented single crystal samples would permit the requisite three sets of optical constants to be extracted. This tough job was accomplished by T. Steyer[81], who measured almost-normal-incidence reflectance through the infrared regions of strong absorption and analyzed the results both by Kramers-Kronig analysis and by Lorentz oscillator fits to the data. The very complete results, comprising three tabulations of n and k, were almost more than most astrophysicists in the field wanted. Some even

stated their preference for "averaged" optical constants, from polycrystalline samples, for example. Almost as soon as the results were distributed through copies of Steyer's dissertation, interest was lost. Why? The absorption, extinction, and emission spectra calculated from such particles had much structure that was too sharp and too numerous to compare favorably with the interstellar 10 μm feature. Even extreme shape effects didn't appear capable of removing the troublesome spectral structure.

Following this development, it occurred to a number of us that the astronomical silicates might have had a hard life during and following their birth in the atmospheres of stars. Perhaps the little things were highly disordered in their crystalline structure — even amorphous or close to it. But how could we make optical-constants measurements on amorphous olivine when our only high-quality bulk samples were the single crystal, gem quality olivine known to gemologists as peridot? The solution adopted by Krätschmer and I was to produce a layer of highly disordered olivine on the surface of oriented single crystals by bombarding them with large doses of heavy ions[82]. The surfaces were lightly repolished after bombardment, and reflectance measurements similar to those of the single crystal work of Steyer were taken. Doing the experiment on three different crystal faces produced identical optical constants (within reasonable uncertainty limits), convincing us that there was no remaining influence of the crystal orientation on the surface layer. Some of the results are shown in Figure 8. With these new optical constants for very badly treated and hence highly disordered olivine, Mie calculations for small particles produced a spectral feature having much more similarity to the interstellar 10 μm feature.

During all this effort to measure optical constants and calculate particulate properties, we wanted to evaluate the whole process by actually making olivine particles from our bulk material and directly measuring extinction. Fortunately olivine, when vaporized in a carbon arc in air, recondenses in particulate form without decomposition. The side-by-side comparison of measured extinction and that calculated from measured optical constants is shown in Figure 9. Although there are appreciable differences, we point out that there have been few tests of this kind made and reported in the open literature. It is rather clear from some of our other work that the decreased height and increased width of the strong peaks is likely due to residual clumping of the particles — that serious thorn in the side of experimenters who aspire to theory-like measurements.

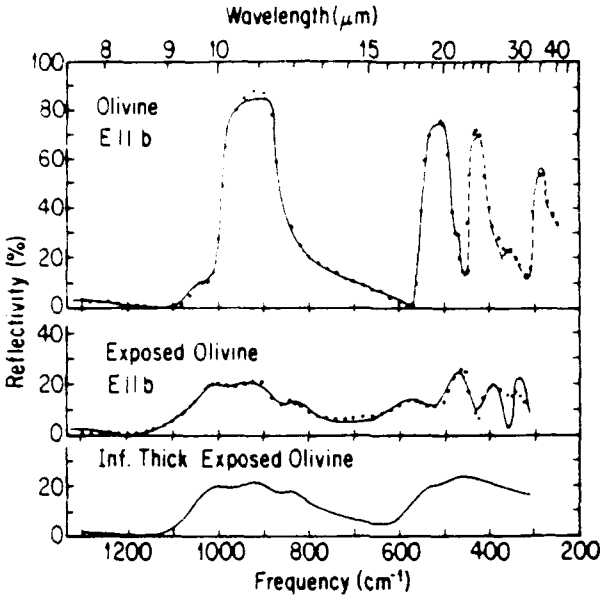

Figure 8. Reflectivity of single-crystal olivine (upper) for the orientation E||b, for a radiation-damaged crystal of olivine (middle), and the calculated reflectivity for an infinite thickness of the radiation-damaged material (lower) using optical constants determined from the middle curve.

And now for further confessions of an experimentalist. It was often true for non-understood reasons that the spectrum of smoke produced in the arc looked more like the smooth hump of interstellar grains than the multi-peaked structure of the smoke in Figure 9. It seemed to make sense at the time that this amorphous-looking olivine smoke could be produced by more violent conditions in the arc -- higher currents and larger gaps. Later, however, when we were desperately trying to make amorphous smoke for quantitative comparisons with our Mie calculations using amorphous olivine optical constants, every experimental variation seemed to produce nothing but the crystalline form of smoke. Clearly there was one or more variables not under our effective control. Yet this lack of being able to control the smoke production at will did not negate the conclusion that there were two distinctly different types of olivine smoke, and that the two different extinction spectra could be reasonably calculated using our two sets of "measured" optical constants. The moral

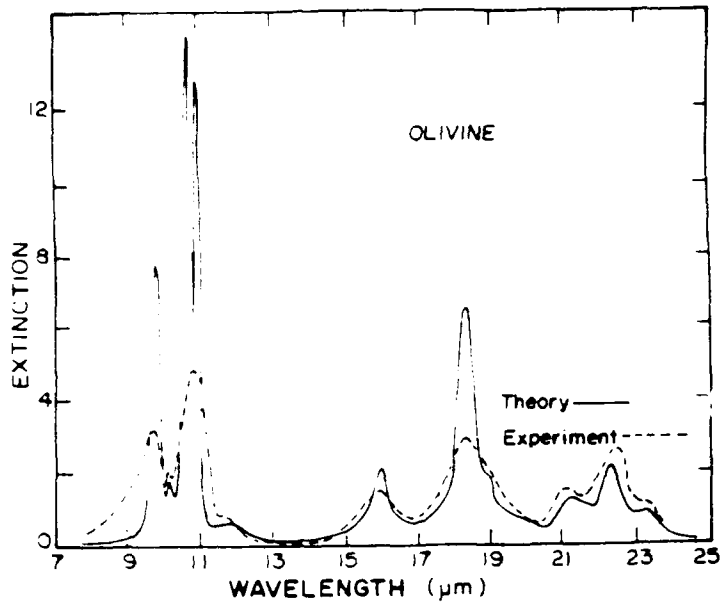

Figure 9. Comparison of experimentally measured extinction for collected smoke particles of olivine with Mie calculations based on measured optical constants for the three directions of single-crystal olivine.

of this story is (again) that small particles may deviate substantially from bulk behavior simply because they are different from available bulk material.

5.3 Silver

In investigations of optical effects in small metal particles, silver has played perhaps the dominant role for several reasons. The surface plasmon for silver particles occurs near the visible region where spectroscopy is readily done, in contrast to most common free-electron metals (aluminum, for example) whose surface plasmon region is in the vacuum ultraviolet region. The optical constants of silver show that it has very low loss ($\epsilon'' = 0.1$) in the surface plasmon region in contrast to gold, for example. Thus very large internal fields can be produced in silver particles. This leads to useful characteristics such as the much studied surface enhanced Raman effect in silver[83], which gives many orders of magnitude enhancement of the Raman signal for scattering from molecules on the surface of silver. Silver also has the advantage of being very stable in contrast to alkali metal particles. Silver does suffer

from one unfortunate disadvantage -- it deviates rather strongly from free-electron (Drude-type) optical behavior, the type which is almost invariably invoked in theory of surface plasmons. In fact, the reason for the desirable shift into the near-visible region is because of the undesirable onset of bound electron effects occurring at lower energy than in some other metals. One sometimes has to take the bad with the good, however. Thus silver has been studied extensively using low-temperature matrix isolation techniques[55,84], in situ gas aggregation techniques[28], and spectroscopy of photosensitive glasses[30,31].

Spectroscopic results from silver isolated in argon and krypton matrices have been collected from several workers and arranged[85] to show a progression from predominantly atoms to dimers to more complex spectra due to larger clusters, and on to the development of small-particle surface plasmon behavior. The plasmon peak first appears broadened and then narrows and begins to shift toward longer wavelengths as the size of the particles increases. None of the techniques of studying the molecule-to-particle transition range are free of problems, however. In low-temperature matrix isolation, surface diffusion of the impinging atoms tends to prevent one from starting with a purely atomic isolated sample[85]. Very low temperature deposition designed to prevent surface diffusion produces amorphous matrices with multiple, nonidentical sites which severely complicate interpretations. The presence of even a single-crystal argon matrix is troublesome due to the shifts and splittings of absorption bands that result. For these reasons we have been experimenting further with the possibility of doing matrix-free studies by creating the clusters and particles in the gas phase and performing the measurements in-situ. Excellent early work has been done along these lines by Broida and coworkers[28,29].

Both scattering and extinction spectra show the dominant surface plasmon band in metals such as silver. Figure 10 shows extinction spectra for silver vaporized from a tantalum boat into 20 torr of helium. The apparatus is constructed so that the source boat can be varied in height in relationship to the collimated white light beam which traverses the rather large chamber. Since the clusters grow from a vapor of atoms into successively larger clusters and particles as they move away from the source, the optical probing as a function of distance will (to some extent) probe the growth process. In the sample probed closest to the source, there is a strong peaking due to atomic silver along with the dominant small-particle peak. In the following two curves, the atomic silver has gone away and the peak starts its expected shift towards the longer wavelength.

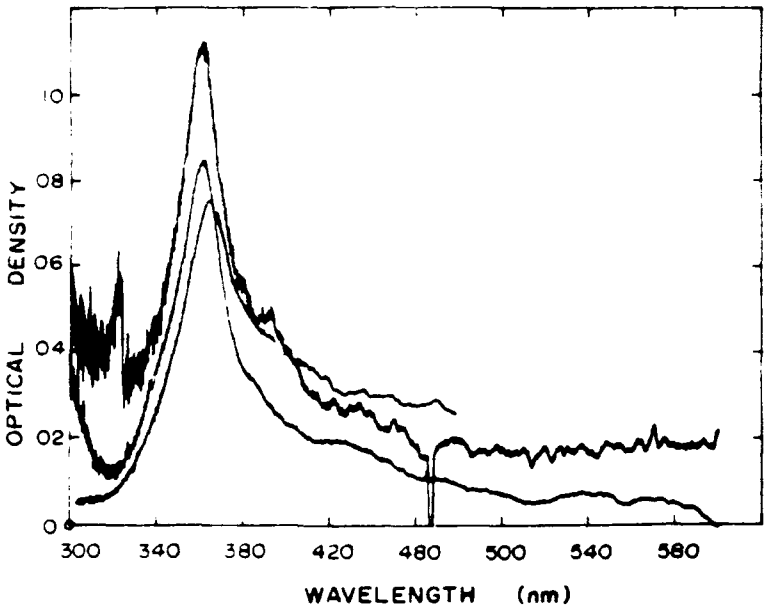

Figure 10. Extinction measured on a cloud of silver smoke particles dispersed in 20 torr of helium gas, for three different source positions. Distances from the source boat to the light beam increase from the upper curve to the lower curve.

To illustrate the rather extreme distortions that can occur when spectroscopy is done "the easy way," that is by collecting particles on a transparent substrate for measurement, we show the results of one run in which a collection on a substrate was taken during a spectral extinction run (Figure 11). This was not a particularly ideal run for production of small particles. Additional absorption in the 4000 to 6000 Å region signals some larger aggregates of particles in the gas-phase measurements. By contrast, however, the collected sample shows a plasmon peak shifted entirely into the visible and greatly broadened. Such is the sensitivity of even loose aggregation on the optical spectra in this region. It should not be inferred that our carbon smoke samples collected on substrates (Section 5.1) are this bad, however. In silver, the critical negative ϵ' region extends from about 3000 Å through the visible and the entire infrared, while for graphite (E c) only a restricted range of negative ϵ' occurs.

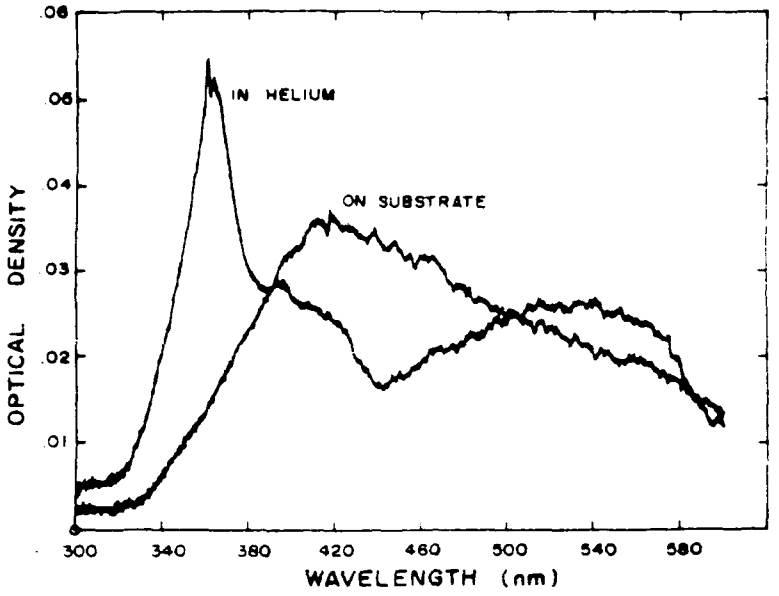

Figure 11. Comparison of extinction measurements on silver smoke in situ in the helium gas with a sample of the same particles collected and measured on a transparent substrate.

Extinction measurements suffer from the fact that they give averaged properties of the smoke particles along the entire path length, over which the particles may vary considerably in shape and size distributions. In principle, scattering measurements have the advantage of being able to probe the smoke chamber's volume selectively, since the scattered light signal comes from the volume formed by the intersection of the collimated incident beam and the detector field of view. This scattering volume can be confined to 1 cm^3 or less. This raises the possibility of probing into spatial regions where different sizes are dominant. Initial work along these lines was done by Eversole and Broida[28], whose system did not permit probing the smoke cloud spatially in three dimensions, however. Some early efforts in our laboratory to scan the surface plasmon peak in scattering at various positions is shown in Figure 12. In the bottom part of the figure, scattering is dominated by scattering from silver atoms along with a strong surface plasmon peak. In the other two cases, the peak shows no atomic scattering, and reveals the shift and broadening of the peak as particle size increases. When developed to its potential, it may be that this technique of probing cluster-particle growth in situ in the gas phase may bring experimental results to bear

on the complicated theoretical problem of particle growth in its various stages of atomic vapor clustering, particle nucleation, particle growth, and particle aggregation[87,88].

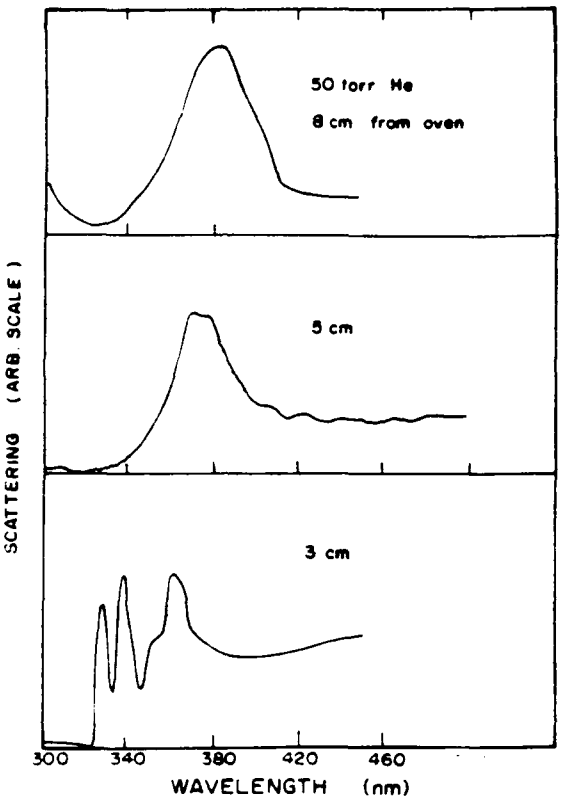

Figure 12. Scattering measurements taken at 45° to the incident beam from a cloud of silver particles supported in helium gas. The different distances from the source boat to the light beam are shown, increasing from bottom to top.

6. SUMMARY: WHEN ARE OPTICAL CONSTANTS OF BULK MATERIAL VALID?

Having set out to answer the question, when are optical constants of bulk matter applicable to small particles, we now give the following brief outline as an answer.

1. When the bulk optical constants are measured accurately: that is, when the bulk n and k are correct.
2. When the small particle is in the same homogeneous state of crystallinity or amorphousness as the bulk.
3. When the particle is isolated sufficiently from other particles.
4. When the particle size is large enough that the following are true:
   a. The bulk crystal structure and lattice constant are achieved.
   b. The ratio of the number of surface atoms to bulk atoms is small.
   c. There are no appreciable quantum size effects.
   d. Energy bands are developed to bulk characteristics.
   e. Damping of free-electron oscillations is not determined by particle size.

The items in point 4 are the ones usually contemplated when applicability of bulk optical constants are questioned. However, we have listed first the points 1-3, only partly with tongue in cheek, since these are the problems which most often give rise to apparent contradictions between bulk and small-particle characteristics. They have been the subject of much of the discussion in this chapter.

Point number four, of course, lists some of the reasons for breakdown of bulk optical constants at small size. Clearly there is no single, small size at which the breakdown occurs. Condensed matter is too varied, and the complex collections of electronic and vibrational excitations in solids are affected differently by decreasing size. Optical properties of the two main classes of solids -- metals and insulators -- react differently, as do excitations in different energy ranges. Although it would take several figures to summarize in any complete way the situation for the several classes of solids and the different spectral regions, we have chosen the case of the surface plasmon region of a metal to summarize the effect of changing size. Martin[89], for example, has used his infrared data to show the development of vibrational structure into surface phonon modes in LiF. Our summary thoughts are shown in Figure 13. The figure represents no particular metal, although we have been guided by the extensive results for silver. In a sense this is a thought experiment, but based on the presently available understanding gained by both experiment and theory.

The game can be played in either direction, by imagining bulk crystals that are successively cleaved to form smaller and smaller particles finally reaching molecular and atomic size, or by envisioning bulk solids being made up from isolated atoms which cluster to form molecular clusters, then small particles which grow ultimately to

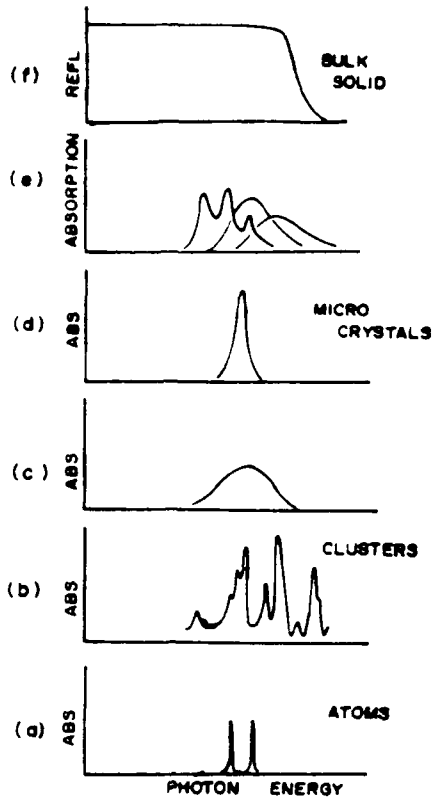

Figure 13. Summary of the development of optical properties of a metal from free atoms through increasingly larger particles to bulk.

become bulk solids. These two mental approaches correspond to two distinct directions our experimental program has taken over the years in attempting to understand the transition. For a long time we naively thought we could disperse the bulk state into fine enough, isolated particles to get at the interesting small-particle effects. After years of partial success, we decided to go to the other extreme and attempt to build up particles from isolated atoms and molecules.

In the development with increasing size of the typical metal of Figure 13, it is likely that no one would be misled into thinking that optical properties of isolated atoms and small molecular culsters would be the same as the bulk metal properties. However, the surface plasmon peak which dominates the spectrum in (d) for particles of the order of 100 Å diameter is not obviously bulk-like. Nevertheless, this feature is easily deriveable from bulk optical constants using (for example) Rayleigh scattering theory. As the particle size increases from this mid-sized region there is a shift, broadening and splitting of the surface plasmon band that has been known since the

time of Gustav Mie and is well characterized by the theory which often carries his name. Thus, the dominant features of small metal particles are all characterized within the bounds of bulk optical constants. A similar thing could be said about the splitting and broadening of the peaks when nonspherical shapes occur. Optical constants remain the same, although calculations may become considerably more difficult.

As one imagines going downward from the approximately 100 Å size of Figure 13(d), shifts and broadening of the surface plasmon peak also occur. The details are in considerably more dispute. Damping of the surface plasmon, either by classical limitation of the mean free paths due to particle boundaries or due to quantum effects arising from discreteness in the density of electron states are thought to cause these effects. Whether quantum or classical, they must be classed as deviations from bulk optical constants.

It seems clear then that, over most of the range of "small particles," optical constants properly measured on bulk material are adequate for describing the optical properties of the small particles, when appropriate theory is used. In order to help us give our bottom-line size estimate of where bulk optical constants begin to fail, we quote a few statements from several authors active in this field, who have had the courage to make definitive statements. Kolb[90] states, "when a metal cluster contains several tens of atoms or more we assume the band structure to be essentially the same as the respective bulk." Regarding clusters of carbon or supposed molecules resembling them found in interstellar space, Tielens and Alamandola[91] proffer, "The metal-to-nonmetal transition in the optical properties of amorphous carbon occurs around an aromatic domain size of about 50 Å ." Regarding the semiconductors that have been studied extensively by their group, Brus et al.[40] state, "The 100 Å diameter and larger crystals show bulk behavior. It is probable that, with high resolution, deviations from bulk behavior just above the band gap would be seen even above 200 Å . However, in 'medium'-sized crystals, typically 40-50 Å, the apparent absorption edge begins to shift to blue, as shown in the figure, at low resolution. For 'small' crystallites, typically of 20-30 Å diameter, the blue shift is more than 1 electron volt."

We therefore conclude that a good working number for the size at which small particles begin to deviate appreciably from bulk optical constants is

50 Å .

Part II

DETAILS OF NON-AGGLOMERATED PARTICLE SPECTROSCOPY

7. INTRODUCTION

Low temperature matrix isolation spectroscopy is a technique that has been used for a number of years by molecular chemists to study absorption spectra of atoms and short-lived molecules. By trapping the molecular species in a crystal of solid rare gas, chemical combination can be avoided so that absorption in the molecules can be measured at leisure. Monographs on this popular technique have been written by Meyer[25] and Moskowitz.[26] Although extensive investigations of simple molecules have been done, chemists have generally been interested in avoiding the large clusters. These are precisely the clusters we have been interested in. The idea has been to produce a sufficient density of atoms in the matrix, and then slowly anneal the matrix by raising the temperature to promote diffusion and enhanced clustering. The hope was that we could go from single atoms to clusters of 2,3,4, ... to very small solid particles. Thus we could bridge the gap continuously between molecular and solid state spectroscopy. Since both electronic absorption in the visible and uv and vibrational absorption in the infrared are of interest, the experimental system could look at the same sample with both types of spectrometers. In Paragraph 8 we describe the experimental apparatus developed and some of the representative results.

Matrix isolation spectroscopy has the great value that large and highly reactive clusters can be isolated for leisurely study by spectroscopic techniques. However, it has the unavoidable disadvantage that the matrix introduces shifts and splittings of the absorption bands, which complicates the interpretation. Because of these complications we considered it important to attempt to do similar spectroscopy of growing clusters and small particles in the gas phase. Although this was not included in the original proposal, it was accomplished with no further funds. The experimental system developed to do gas phase spectroscopy in the visible and ultraviolet is described in Paragraph 9.

8. MATRIX ISOLATION SPECTROSCOPY

8.1 Experimental Apparatus

In accord with the aims of the proposed work, it was necessary to bring both visible and infrared spectrophotometry to bear on the cryogenically cooled sample. Since there are no commercially available spectrophotometers that span the entire range from vacuum ultraviolet to far infrared and, if there were, the cost would doubtless be greater than the entire three-year budget for this grant, we have mated

two instrument systems that were available in our laboratory. The result is shown schematically in Figure 14. A McPherson 235, Seya Namioka monochromator was used as the basic uv and visible monochromator. With a 600 lines/mm grating, it can span the range from about 90 nm to 600 nm using an appropriate source. For most work between 190 and 600 nm, a high-pressure Xenon lamp was used, supplemented at times with a Hinteregger-type gasseous discharge lamp using H_2 for vacuum ultraviolet work or a tungsten lamp for a better continuum in the visible. The beam emerging from the exit slit of the monochromator passes through the cold finger of the Oxford Instruments Corporation continuous-flow cryostat, which holds a saphire (or other) substrate onto which the matrix gas is flowed. A photomultiplier tube coated on its envelope with sodium salicylate serves as the detector. For infrared spectroscopy, the cryostat can be rotated 90 degrees into the beam of a focused globar. After going through the sample, the beam enters the entrance slit of a monochromator constructed from the insides of a Beckmann IR7/11 series spectrophotometer. The interchangeable prism-grating module in this sytem makes possible spectroscopy from 2 micrometers to about 200 micrometers. For most of the work, an HgCdTe detector, cooled by liquid nitrogen, was used. A liquid-helium-cooled germanium bolometer was also available for far infrared.

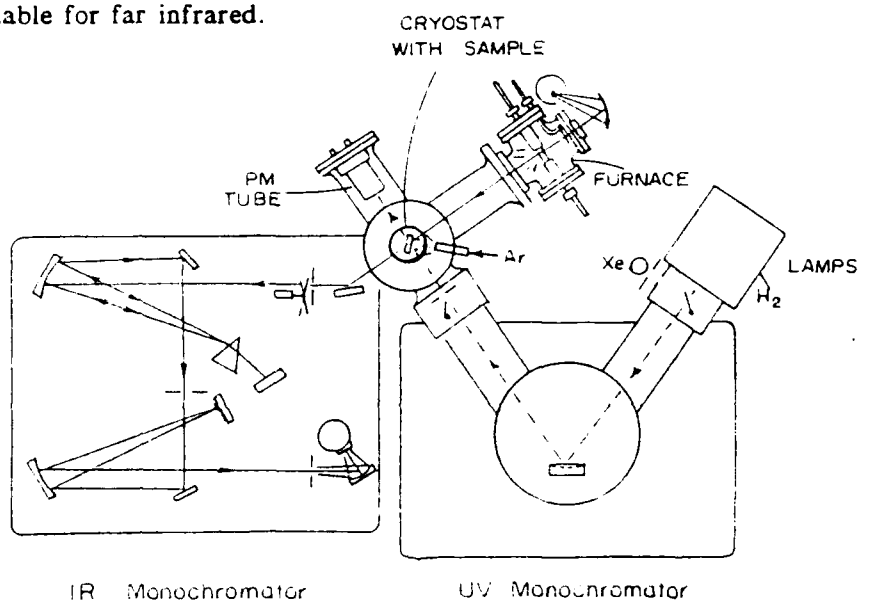

Figure 14. Top view of the apparatus developed for doing matrix isolation spectroscopy on the same sample in the vacuum ultraviolet, visible, and infrared wavelength ranges.

In a typical run in which both ir and visible are measured, the cryostat is first positioned with the substrate facing the sample oven. With the substrate at about 10

K, argon gas is flowed onto the saphire substrate. Thicknesses of the matrix can be calibrated using interference fringes in the solid argon matrix. Next, the oven is activated to evaporate the species under study into the flowing gas stream. When a suitable sample has been achieved, the cryostat can be rotated to allow the visible-uv beam to transit the sample or kept in the original position for ir spectroscopy.

8.2 Some Results on Metal Clusters

By the time the equipment just described was perfected, a good bit of work had already been done in matrix isolating pure metals, especially silver[54,84,85,90]. Wishing to investigate both electronic and vibrational properties, we turned to systems of mixed metal aggregates such as silver and sodium. The following idea was suggested by then-graduate-student Kent Pflibsen. He noted that, because pure metal clusters do not have an appreciable dipole moment to couple to the infrared electromagnetic wave, it might be impossible to do vibrational spectroscopy on clusters of silver (for example). However, by co-evaporating two different metals into the matrix, one could possibly alloy mixed clusters of metals which would have a dipole moment induced by differing electronegativities on the two metal atoms. This astute suggestion was tried successfully on several different clusters of metals. The visible-uv spectra were fairly easily interpreted on the basis of previous work on the different pure metals and new calculations done by Pflibsen. The complete results are reported in the Ph.D. thesis of Pflibsen,[93] with a less complete version published in the Proceedings of the 1983 International Conference on Clusters and Small Particles.[94]

Representative results from the work on mixed metal clusters are shown in Figures 15 and 16. The electronic spectrum of Figure 15 clearly shows the silver atom absorption lines along with the sodium dimer. (The Na monomer is not included in the wavelength range of this plot.) These bands were well-known from previous work. The new mixed metal bands along with their identifications are also pointed out. In this case, which is fairly representative of the other mixed metal systems studied, clusters of 2, 3, and 4 atoms could be identified, but no more. Attempts to follow the development of even larger clusters by additional annealing led only to the development of very broad absorption bands characteristic of plasmon absorption in poorly defined solid particles. The corresponding development of the solid state, phonon absorption band in the AgNa clusters is shown in Figure 16, where two different levels of annealing are shown in addition to the as-depositied sample spectra. Within the spectral range shown, only 2 and 3 atom clusters are identifiable along with the development of the phonon band. One substantial success of this experiment was the ability to identify the absorption feature of the microcrystals of mixed metal.

The disappointment in not being able to follow the development of larger clusters in the transition to the solid state is characteristic of what other workers have also encountered (see references 35,55,84,85,89).

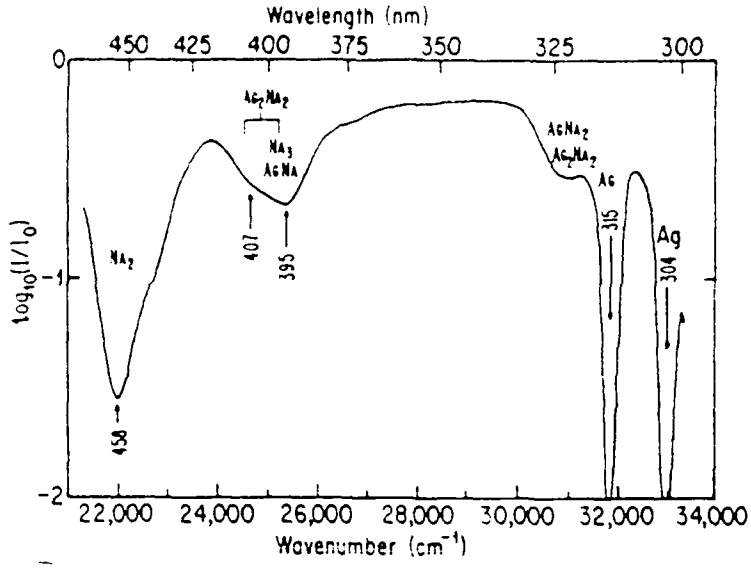

Figure 15. Transmission spectrum of AgNa clusters in the 21000 to 34000 inverse cm (470 to 300 nm) spectral region. Appearing on the figure are the experimentally determined peak positions, designated by arrows, and the cluster identifications derived from the fitting procedure based on theoretical calculations.

8.3 Some Results on Carbon

In addition to being a cosmically interesting solid (see Section 5.1), carbon is of continuing interest to the Army's program of obscuration. Carbon has one of the higher values of extinction per unit volume in the infrared, and extinction by graphite can be further optimized using shape effects such as occur in platelets or needles. Although carbon was not an element mentioned prominently in the proposal for the present work, a significant amount of work has been devoted to carbon clusters. The reason is that carbon, in contrast to most other metals and semimetals, vaporizes with a majority of three atom clusters. This gives it a head start in the game of producing large molecular clusters for matrix isolation. Indeed, when our first matrix isolation experiments were done on the vapor from incandescent carbon, in collaboration with W. Krätschmer, a rich spectrum of absorption bands occurred, as in Figure 5. Annealing of the solid argon matrix produced further growth of some bands accompanied by decrease of some of the original bands. Despite considerable past

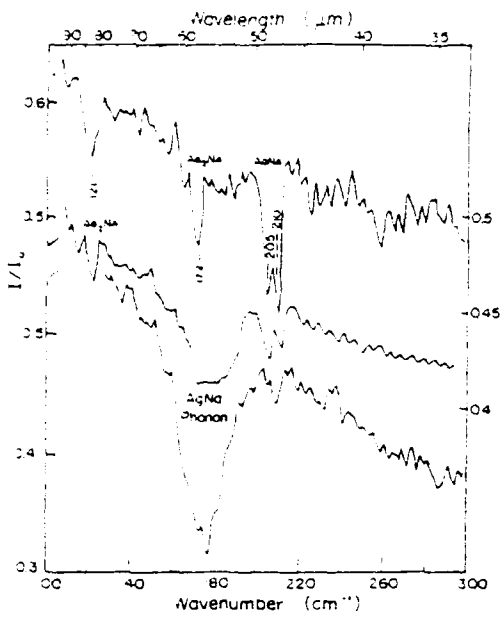

Figure 16. Three transmission spectra for AgNa molecular clusters and small particles in the 40 to 440 inverse cm (250 to 22.5 micrometer) spectral range. The degree of aggregation of the metals increases from the top (small molecular clusters) to the bottom (small particles). Appearing on the figure are the experimentally determined peak positions designated by arrows and the cluster identification derived from the fitting procedure based on theoretical calculations. The left-hand scales apply to the top and bottom curves, respectively, and the right-hand scale applies to the middle curve.

work on carbon, these results have not previously been reported in the literature. The results of the original experiment done in Heidelberg have since been repeated many times at both Heidelberg and Tucson using the apparatus of Figure 14. The original interpretation of the bands[64] suggested that they were due to clusters ranging from the well-known C3 (with a band near 410 nm) to about C9. Considerable further work has been done in an attempt to more firmly identify the clusters responsible for the plethora of absorption bands, with very little success. The problem seems to be that the state of the art in ab initio calculations of large clusters is still uncertain enough that different theorists even predict different ground state configurations for a given cluster. Uncertainties in calculated energies are large enough that the calculations are not able to permit identification of the bands. Nevertheless, it appears that our case of carbon has permitted larger clusters to be aggregated and studied spectroscopically than any other solid yet studied in matrix isolation spectroscopy.

In view of the failure of theorists to be of much help at the present time, we have turned to an attempt to identify the clusters of carbon by use of combined infrared (vibrational) and visible (electronic) spectroscopy. Although the visible spectra of carbon clusters had not previously been published prior to this work,

Weltner and colleagues had done nice work on the infrared spectra of carbon clusters prepared and isolated in a similar way.[95] He used a combination of theory and experiments employing isotopic substitution of the carbon atoms to attempt identification of the infrared bands. In addition to our being able to draw from the work of this experienced and respected worker, the vibrational bands should be a bit easier to work with theoretically, since only the electronic ground state is of concern, in contrast to electronic transitions which also involve electronic excited levels. Unfortunately, we were not able to bring this work to a conclusion before the end of the grant. One of the difficulties involved has been the quite different absorption strengths of the infrared and visible bands, which necessitates much more carbon for good spectral definition in the case of the infrared bands. Nevertheless preliminary results showing spectra of both infrared and ultraviolet regions for the sample matrix isolated carbon samples are available. The work is continuing as the Ph.D. thesis work of Joe Kurtz.

Since we have been more successful in producing large clusters in the case of carbon than in any other system we (and perhaps anyone else) have studied, it was important to try our best to increase the cluster size continuously until solid state behavior would set in. This bulk behavior should be recognizable in the case of carbon by the surface plasmon oscillation of pi electrons in the small solid particles. The characteristic band occurs at about 220 nm. Figure 17 shows the results of a increasing the carbon concentration in proportion to the amount of argon matrix material. Other studies were done in which a constant carbon concentration was annealed to increasingly greater degrees. The results of both experiments were similar to those given in Figure 17. One notices the decrease of the C3 band (407 nm) to nearly nil, the initial increase of the 450 nm band and other bands attributed to larger carbon clusters, followed by their merging into the continuum. What does not happen, however, is an increasing complexity of the bands as growth towards the solid state occurs. All of the same bands that have appeared at the 3.6 per cent level persist, with no new ones apparent. Another disappointing feature is that, although a broad, solid state-like absorption feature develops centered at about 300 nm, it is much broader than the expected surface plasmon band in any form of carbon existing as isolated small particles. Our speculation is again that a messy tangle of percolation channels have developed as the concentration is increased, leading to a tangled web of carbon in the matrix, rather than the isolated solid particles we had desired to grow from increasingly larger clusters. The behavior is similar to that already discussed above, which has been observed in other matrix isolated systems.

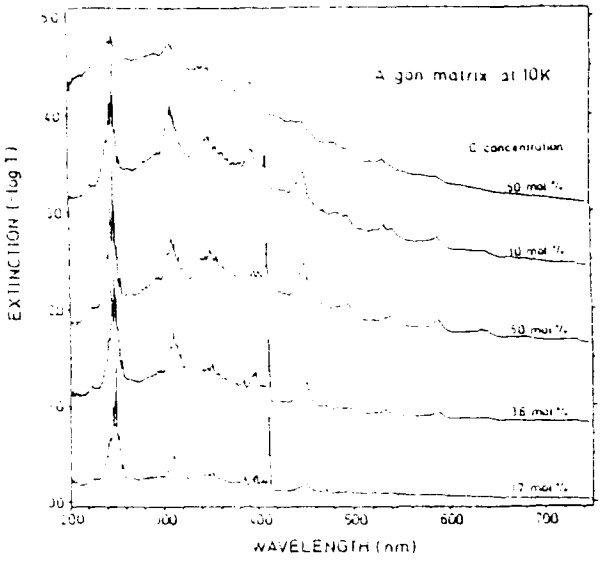

Figure 17. Matrix isolation spectra of increasing proportions of carbon to argon showing the development of the solid state feature from molecular features. Similar results occur with moderate concentrations of carbon and increasingly severe annealing.

9. GAS PHASE SPECTROSCOPY

Because of the unavoidable shifts and splittings of molecular absorption bands in frozen gas matrices, it was deemed desirable to attempt to do spectroscopy of molecular clusters growing into small particles in the gas phase.

9.1 Equipment Developed

Many studies of the formation of metal particles by vaporization of metals into inert gas environments have been carried out, especially by the Japanese workers. While the production of such smoke clouds lends itself nicely to optical probing, most of the studies have been non-optical, aiming rather at investigating the size and shapes produced under varying conditions by means of electron microscopy. A notable exception was the work of Prof. Broida and students at Santa Barbara (see references 28 and 86, for example), which program essentially ceased at the death of Broida. Although this experiment was not proposed in the written proposal for the current grant, it seemed important to pursue this possibility after the limitations of the low-temperature matrix isolation technique began to be apparent.

The experimental system constructed is shown schematically in Figure 18. A cylindrical smoke chamber of about 50 cm diameter and 60 cm in height is mounted on an oil diffusion pumped high-vacuum system, with provision for varying the pressure of inert gases in the chamber. A highly collimated light beam produced from

a high-pressure xenon lamp traverses the chamber through one pair of a series of windows. The vaporization oven for producing metal smoke is mounted on a high-vacuum mechanical feedthrough to permit the relative position of the vapor source to be varied in relation to the light beam. In this way one can optically probe from very close to the vapor source, where atomic vapor has not yet begun to nucleate and grow clusters, to a little farther where molecular clusters form, to increasing distances from the source where small solid particles form and grow.

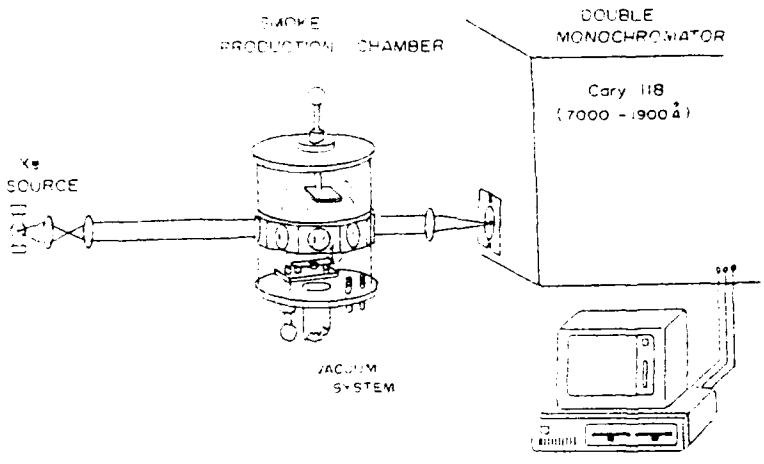

Figure 18. Schematic diagram of the system developed to do wavelength-dependent extinction and scattering measurements at varying positions in a cloud of metal smoke.

The heart of the present system is a dedicated Cary 118 double prism spectrophotometer, which was acquired in perfect working condition at nominal cost from the University of Arizona Medical School. It was adapted for computer control by an IBM PC system, and modified optically to permit extinction measurements to be made using the collimated, external light beam and proper entrance optics for measuring extinction. By moving the light beam either 45 or 90 degrees from the position shown, spectral measurements of scattering can also be made as a function of spatial position in the smoke cloud. The range of the combined extinction and scattering spectrometer is from 190 to 700 nm. We proudly point out that there is no commercial instrument on the market that does what this instrument does, and if it were contracted for, it would surely cost $100,000 or more. Yet we have managed to bootleg this project along on the present grant, in addition to the proposed work, at a total cost for the entire project of well under $100,000 of actual expenditure (after

subtracting overhead).

9.2 Representative Results

To date, the metal smokes that have been investigated in the scattering-extinction spectrometer are magnesium, sodium, and silver, with the majority of the work focusing on silver. The reason is that silver forms a relatively unreactive type of particle and has its main surface plasmon absorption in the convenient near ultraviolet range at about 360 nm. Figures 10 and 12 of Part I have shown representative extinction and scattering spectra (respectively) for silver smoke. Both types of spectra show the surface plasmon band with a width that is very similar to that obtained from calculations on isolated single particles. This is in contrast to almost all reported matrix isolation spectra of small silver particles which show a much broadened surface plasmon band, probably the undesirable effect of clustering of particles. Silver monomer absorption and scattering is also obvious in the two examples. In some spectra there is marginal evidence for silver dimers and perhaps trimers. As the optical probe is moved higher above the source, particles of increasing size can be studied and sized in-situ by means of the predictable shift of the surface plasmon band (Fig. 10). Even farther from the source there occurs the inevitable clustering of individual solid particles into clustered chains. The precursor of a chain is an aggregation of two particles, just as the precursor of a large molecular cluster is a dimer. Although the theoretical calculation of spectral properties of a cluster of two or more metal particles is in the early stages, it appears promising that one can identify the new positions of the shifted surface plasmon band for a cluster of two particles. Spectra of silver particles obtained farther from the source than those of Figure 10 do indeed show additional bands which eventually may be shown to be due to two-particle clusters.

In summary, it appears that spectroscopic probing of a developing smoke system may be able to monitor (1) the density of monomers, (2) the development of small (two or three atom) molecular clusters, (3) the development and growth of small solid particles, and (4) the initial clustering of the individual particles. Obviously a large amount of further work will be required to exploit the virtues of this system, for which further funding is being sought. In comparison to matrix isolation, it may not be possible to produce clusters that are quite as large in the gas phase because of the rapidity with which they pass through the large cluster region. However, the superior isolation of the growing metal particles and the ability to probe the growing medium spatially make the gas aggregation technique a very promising tool for future work. We expect it will provide important direct information regarding the

complicated processes of nucleation, growth and clustering of particles formed from the vapor.[99]

9.3 Future Plans

In addition to exploiting the apparatus of Figure 17 for metal smokes, we desire to explore the interesting system of carbon particles, which has proven so interesting in the matrix isolation work. Unfortunately, in contrast to the metal smokes, carbon does not permit a stable smoke cloud to be formed easily. This is primarily because of the very high temperatures required to produce vaporization of carbon. In order to do carbon smoke effectively, we are pursuing a modification of the system in which the conventional scanning spectrometer is replaced with a rapid scanning system consisting of an array detector with image intensification. This should permit the spectrum to be acquired in a small fraction of a second rather than the typically 10 sec required with the present system. Thus the spectrum of a puff of smoke such as carbon can be recorded.

REFERENCES

1. Bohren, C. F. and Huffman, D. R., Absorption and Scattering of Light by Small Particles, Wiley, New York (1983).

2. Weaver, J. H., Krafka, C., Lynch, D. W., and Koch, E. E., "Optical Properties of Metals," Physik Daten 18-1 (1981).

3. Palik, E. D. (Ed.), Handbook of Optical Constants of Solids, Academic Press, New York (1985).

4. Mitra, S., "Optical Properties of Nonmetallic Solids," in Handbook of Optical Constants of Solids, E. D. Palik (Ed.), Academic Press, New York (1985), pp. 214, 230-231.

5. Stern, F., "Elementary Theory of the Optical Properties of Solids," Solid State Physics 15, 299-308 (1964).

6. Cardona, M., "Optical Constants of Insulators: Dispersion Relations," in Optical Properties of Solids, S. Nudelman and S. S. Mitra (Eds.), Plenum, New York (1969), pp. 137-151.

7. Aspnes, D. E., "The Accurate Determination of Optical Properties by Ellipsometry," in Handbook of Optical Constants of Solids, E. D. Palik (Ed.), Academic Press, New York (1985), pp. 89-112.

8. Reference 3, p. 5.

9. Reference 2, p. 18.

10. Huffman, D. R., "Interstellar Grains: The Interaction of Light with a Small-Particle System," Adv. Phys. 26, 129-230 (1977).

11. Aspnes, D. E., Reference 7, p. 110.

12. Mie, G., "Beitrage zur Optik truber Medien speziell kolloidaler Metallösungen," Ann. Phys. 25, 377-445 (1908).

13. Kerker, M., The Scattering of Light and Other Electromagnetic Radiation, Academic Press, New York (1969).

14. Wehl, W. A., Colored Glasses, The Society of Glass Technology, Sheffield, England (1951).

15. Hagemann, H. J., Gudat, W., and Kunz, C., "Optical Constants from the Far Infrared to the X-ray Region: Mg, Al, Cu, Ag, Au, Bi, C, and α-Al_2O_3," Deutsches Elektronen-Synchrotron DESY SR-74/7 (1974).

16. Reference 1, pp. 327 and 335-336.

17. Reference 1, p. 145.

18. Reference 1, pp. 353-356.

19. Ruppin, R. and Englman, R., "Optical Phonons of Small Crystals," Rep. Prog. Phys. 33, 149-196 (1970).

20. Genzel, L., "Aspects of the Physics of Microcrystals," Festkörperprobleme (Advances in Solid State Physics) XVI, 183-203 (1974).

21. Steyer, T. R., Day, K. L., and Huffman, D. R., "Infrared Absorption by Small Amorphous Quartz Spheres," Appl. Opt. 13, 1586-1590 (1974).

22. Reference 1, pp. 360-362.

23. Huffman, D. R., "Optical Absorption Studies of Surface Plasmons and Surface Phonons in Small Particles," Festkörperprobleme (Advances in Solid State Physics) XXIII, 49-75 (1983). See also reference 1, p. 367.

24. Fuchs, R., "Theory of the Optical Properties of Ionic Crystal Cubes," Phys. Rev. B11, 1732-1740 (1975).

25. Meyer, B., Low Temperature Spectroscopy, Elsevier, New York (1971).

26. Moskovitz, M. and Ozin, G. A. (Eds.), Cryochemistry, Wiley, New York (1976).

27. Rossetti, R., Hull, R., Gibson, J. M., and Brus, L. E., "Excited Electronic States and Optical Spectra of ZnS and CdS Crystallites in the 15 to 50 Å Size Range: Evolution from Molecular to Bulk Semiconducting Properties," J. Chem. Phys. 82, 552-559 (1985).

28. Eversole, J. D. and Broida, H. P., "Size and Shape Effects in Light Scattering from Small Silver, Copper, and Gold Particles," Phys. Rev. B15, 1644-1655 (1977).

29. Hecht, J., "Optical Properties of K Smoke Particles from 480-620 nm," J. Opt. Soc. Am. 70, 694-697 (1980).

30. Stookey, S. D., Beall, G.H., and Pierson, J. E., "Full-color Photosensitive Glass," J. Appl. Phys. 49, 5114-5123 (1978).

31. Doremus, R. H., "Optical Properties of Small Gold Particles," J. Chem. Phys. 40, 2389-2396 (1964).

32. Doyle, W. T., "Absorption of Light by Colloids in Alkali Halide Crystals," Phys. Rev. 111, 1067-1077 (1958).

33. Brown, W. L., Freeman, R. R., Raghavachari, K., and Schlüter, M., "Covalent Group IV Atomic Clusters," Science 235, 862 (1987).

34. Ibid., 864.

35. Martin, T. P., "Alkali Halide Clusters and Microcrystals," Phys. Reports 95, 167-199 (1983).

36 Tomanek, D. and Schlüter, M., "Calculation of Magic Numbers and the Stability of Small Si Clusters," Phys. Rev. Lett. 56, 1055-1058 (1986).

37. Kroto, H. W., Heath, J. R., O'Brien, S. C., Curl, R. F., and Smalley, R. E., "C60: Buckminsterfullerene," Nature (London) 318, 162-163 (1985).

38. Zhang, Q. L., O'Brien, S. C., Heath, J. R., Lin, Y., Curl, R. F., Kroto, H. W., and Smalley, R. E.,"Reactivity of Large Carbon Clusters: Spheroidal Carbon Shells and Their Possible Relevance to the Formation of Morphology of Soot," J. Phys. Chem. 90, 525-528 (1986).

39. Spain, I. L., "Electronic Transport Properties of Graphite, Carbons, and Related Materials," Chemistry and Physics of Carbon 16, 119-304 (1981).

40. Brus, L., "Electronic Wave Functions in Semiconductor Clusters: Experiment and Theory," J. Phys. Chem. 90, 2555-2560 (1986).

41. Rossetti, R., Nakahara, S., and Brus, L. E., "Quantum Size Effects in the Redox Potentials, Resonance Raman Spectra, and Electronic Spectra," J. Chem. Phys. 79, 1086-1088 (1983). See other references in 40.

42. Fojtik, A., Weller, H., Koch, U., and Henglein, A., "Photochemistry of Colloidal Metal Sulfides. 8. Photo-Physics of Extremely Small CdS Particles: Q-State CdS and Magic Agglomeration Numbers," Ber Bunsenges. Phys. Chem. 88, 969-977 (1984).

43. Weller, H., Koch U., Gutiérrez, M., and Henglein, A., "Photochemistry of Colloidal Metal Sulfides. 7. Absorption and Flourescence of Extremely Small ZnS Particles (The World of the Neglected Dimensions)," Ber. Bunsenges. Phys. Chem. 88, 649-656 (1984).

44. Reference 43, p. 650.

45. Ostwald, W., Die Welt der Vernachlässigten Dimensionen, 4th Ed., Steinkopf, Dresden (1920); English Translation, An Introduction to Theoretical and Applied Colloid Chemistry: The World of Neglected Dimensions, Wiley, New York (1917).

46. Kreibig, U. and Genzel, L., "Optical Absorption of Small Metallic Particles," Surf. Sci. 156, 678-700 (1985).

47. Kawabata, A. and Kubo, R., "Electronic Properties of Fine Metallic Particles. II. Plasma Resonance Absorption," J. Phys. Soc. Jpn 21, 1765-1772 (1966).

48. Genzel, L., Martin, T. P., and Kreibig, U., "Dielectric Function and Plasma Resonances of Small Metal Particles," Z. Physik B21, 339-346 (1975).

49. Kraus, W. A. and Schatz, C. C., "Plasmon Resonance Broadening in Small Metal Particles," J. Chem. Phys. 79, 6130-6139 (1983).

50. Gor'kov, L. P. and Eliashberg, G. M., "Minute Metallic Particles in an Electromagnetic Field," Sov. Phys. JETP 21,940-947 (1965).

51. Doyle, W. T. and Agarwal, A., "Optical Extinction of Metal Spheres," J. Opt. Soc. Am. 55, 305-309 (1965)

52. Kreibig, U. and von Fragstein, C., "The limitation of Electron Mean Free Path in Small Silver Particles," Z. Phys. 224, 307-323 (1969).

53. Kreibig, U., "Electronic Properties of Small Silver Particles: The Optical Constants and Their Temperature Dependence," J. Phys. F. 4, 999-1014 (1974).

54. Charlé, K.-P., Frank, F., and Schulze, W., "The Optical Properties of Silver Microcrystallites in Dependence on Size and the Influence of the Matrix Environment," Ber. Bunsenges. Phys. Chem. 88, 350-354 (1984).

55. Abe, H., Schulze, W., and Tesche, B., "Optical Properties of Silver Microcrystals Prepared By Means of the Gas Aggregation Technique," Chemical Physics 47, 95-104 (1980).

56. Halperin, W. P., "Quantum Size Effects in Metal Particles," Rev. Mod. Phys. 58, 533-606 (1986).

57. Tanner, D. B., Sievers, A. J., and Buhrman, R. A., "Far Infrared Absorption in Small Metal Particles," Phys. Rev. B11, 1330-1341 (1975).

58. Granqvist, C. G., Buhrman, R. A., Wyns, J., and Sievers, A. J., "Far-infrared Absorption in Ultrafine Al Particles," Phys. Rev. Lett. 37, 625-629 (1976).

59. Devaty, R. P. and Sievers, A. J., "Comment on Gor'kov and Eliashberg's Theory for Far-Infrared Absorption by Small Metal Particles," Phys. Rev. B22, 2123-2126 (1980).

60. Ruppin, R. "Far-infrared Absorption in Small Metallic Particles," Phys. Rev. B19, 1318-1321 (1979).

61. Devaty, R. P. and Sievers, A. J., "Far-Infrared Absorption by Small Metal Particles," Phys. Rev. Lett. 52, 1344-1347 (1984).

62. Gerber, H. and Hindman, E. (Eds.), Light Absorption by Aerosol Particles, Spectrum Press, Hampton, Va. (1982).

63. Turco, O. R., Toon, P. B., Ackerman, T. P., Pollack, T. P., and Sagan, C., "Nuclear Winter: Global Consequences of Multiple Nuclear Explosions," Science 222, 1283-1292 (1983).

64. Krätschmer, W., Sorg, N., and Huffman, D. R., "Spectroscopy of Matrix-Isolated Carbon Cluster Molecules Between 200 and 850 nm Wavelength," Surf. Sci. 156, 814-821 (1985).

65. Alamandola, L. J., Tielens, A. G. G. M., and Barker, J. R., "The IR Emission Features: Emission from PAH Molecules and Amorphous Carbon Particles," in Polycyclic Aromatic Hydrocarbons and Astrophysics, A. Leger and L. B. d'Hendecourt (Eds.), Reidel, Dordrecht (1986).

66. Puget, J. L., Léger, A., and Boulanger, F., "Contribution of Large Polycyclic Aromatic Molecules to the Infrared Emission of the Interstellar Medium," Astron. and Astrophys. 142, L19-L22 (1985).

67. Sato, Y., "Optical Study of Electronic Structure of Graphite," J. Phys. Soc. Japan 24, 489-492 (1968).

68. Philipp, H. R., "Infrared Optical Properties of Graphite," Phys. Rev. A138, 2896-2900 (1977).

69. Private Communication, R. W. Alexander, Jr. and R. J. Bell.

70. Draine, B. T., "Tabulated Optical Properties of Graphite and Silicate Grains," Astrophys. J. Suppl. 57, 587-594 (1985).

71. Max Planck Institut für Kernphysik, Heidelberg.

72. Honig, R. E., "Mass Spectrometric Study of the Molecular Sublimation of Graphite," J. Chem. Phys. 22, 126-131 (1954).

73. Pitzer, K. S. and Clementi, E., "Large Molecules in Carbon Vapor," J. Am. Chem. Soc. 81, 4477-4485 (1959).

74. Slanina, Z. and Zahradnik, R., "MINDO/2 Study of Equilibrium Carbon Vapor," J. Phys. Chem. 81, 2252-2257 (1977).

75. Whiteside, R. A., Krishnan, R., Defrees, J., Pople, J. A., and Schleyer, P., "Structure of C_4," Chem. Phys. Lett. 78, 538-540 (1981).

76. Stephens, J. R., "Visible and Ultraviolet (800-130 nm) Extinction of Vapor-Condensed Silicate, Carbon, and Silicon Carbide Smokes and the Interstellar Extinction Curve," Astrophys. J. 237, 450-461 (1980).

77. Koike, C., Hasegawa, H., and Manabe, A., "Extinction Coefficients of Amorphous Carbon from 2100 Å to 340 μm," Astrophys. Space Sci. 67, 495-502 (1980).

78. Vidano, R. R., Fischbach, D. B., Willis, L. J., and Loehr, T. M., "Observation of Raman Band Shifting with Excitation Wavelength for Carbons and Graphites," Sol. State Comm. 39, 341-344 (1981).

79. Wright, R. B., Varma, R., and Gruen, D. M., "Raman Scattering and SEM Studies of Graphite and Silicon Carbide Surfaces Bombarded with Energetic Protons, Deuterons, and Helium Ions," J. Nucl. Mat. 63, 415-421 (1976).

80. Grossman, L., "Condensation in the Primitive Solar Nebula," Geochim. Cosmochim. Acta 36, 597-619 (1972).

81. Steyer, T. R., "Infrared Optical Properties of Some Solids of Possible Interest in Astronomy and Atmospheric Physics," Ph.D. Thesis, Dept. of Physics, University of Arizona (1974).

82. Krätschmer, W., and Huffman, D. R., "Infrared Extinction of Heavy Ion Irradiated and Amorphous Olivine, with Applications to Interstellar Dust," Astrophys. Space Sci. 61, 195-203 (1979).

83. Chang, R. K. and Furtak, T. E. (Eds.), Surface Enhanced Raman Scattering, Plenum, New York (1982).

84. Welker, T., "Optical Absorption of Matrix Isolated Silver Aggregates and Microcrystals," Ber. Bunsenges. Phys. Chem. 82, 40-41 (1978).

85. Meyer, B., "Spectra of Matrix Isolated Metal Atoms and Clusters," Ber. Bunsenges. Phys. Chem. 82, 24-29 (1978).

86. Mann, M. and Broida, H. P., "Plasma Resonance Scattering Studies of the Formation of Alkali Metal Particles in Inert Gases," J. Appl. Phys. 44, 4950-4955 (1973).

87. Kim, S. G. and Brock, J. R., "Formation of Primary Metal Particles in Evaporation Chambers," J. Appl. Phys. 60, 509-513 (1986).

88. Granqvist, C. G. and Hunderi, O., "Optical Properties of Ultrafine Gold Particles," Phys. Rev. B16, 3513-3534 (1977).

89. Martin, T. P., "Infrared Absorption in LiF Polymers and Microcrystals," Phys. Rev. B15, 4071-4076 (1977).

90. Kolb, D. M., "Matrix Isolation Spectroscopy of Metal Atoms and Small Clusters," in Matrix Isolation Spectroscopy, A. J. Barnes, W. J. Orville-Thomas, A. Müller, and R. Ganfrés (Eds.), Reidel, Boston (1981), p. 468.

91. Tielens, A. G. G. M. and Allamandola, L. J., "Evolution of Interstellar Dust," in Physical Processes in Interstellar Clouds, G. Morfill and M. Scholer (Eds.), Proceedings of a meeting held in Irsee, Germany, August 1986 (in press).

92. Reference 40, pp. 2556-2557.

93. Pflibsen, K. P., "The Vibrational and Electronic Absorption Spectra of AgLi, AgNa, CuLi, and CuNa from Single Molecules to Small Particles," Ph.D. Dissertation, Department of Physics, University of Arizona (1984).

94. Pflibsen, K. P. and Huffman, D. R., "Electronic and Vibrational Spectra of AgNa Molecular Clusters and Small Particles," Surface Sci. 156, 793-799 (1985).

95. Thompson, K. R., DeKock, R. L., and W. Weltner, Jr., "Spectroscopy of Carbon Molecules. IV.," J. Am. Chem. Soc. 93, 4688-4695 (1971).